Reproduction Quality Notice

This document is part of the Air Technical Index [ATI] collection. The ATI collection is over 50 years old and was imaged from roll film. The collection has deteriorated over time and is in poor condition. DTIC has reproduced the best available copy utilizing the most current imaging technology. ATI documents that are partially legible have been included in the DTIC collection due to their historical value.

If you are dissatisfied with this document, please feel free to contact our Directorate of User Services at [703] 767-9066/9068 or DSN 427-9066/9068.

Do Not Return This Document To DTIC

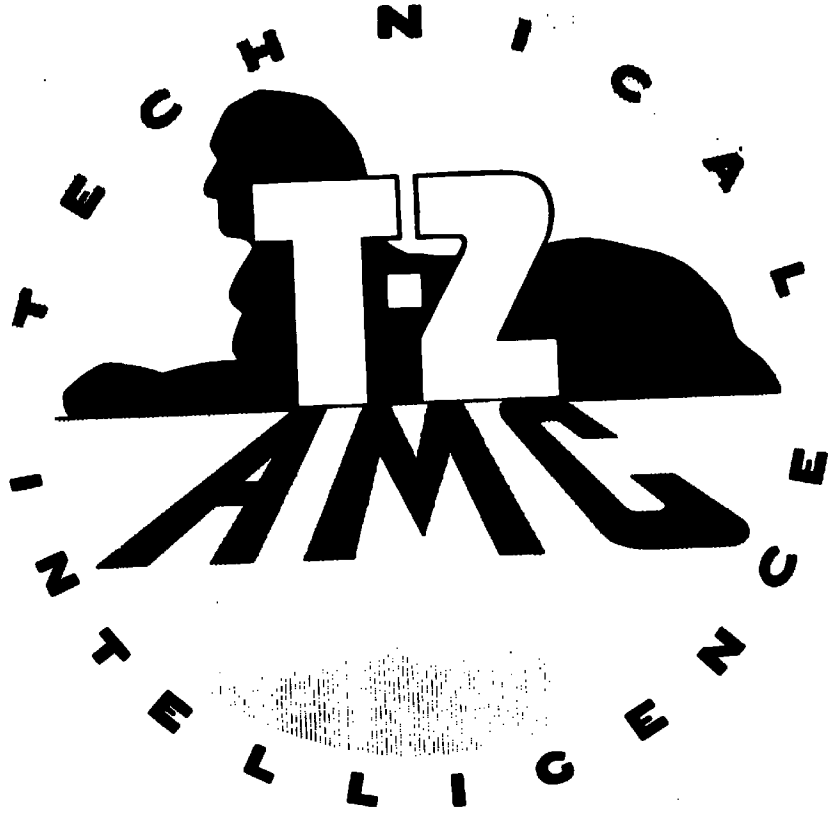

The U.S. GOVERNMENT

IS ABSOLVED

FROM ANY LITIGATION WHICH MAY ENSUE FROM THE CONTRACTORS IN-FRINGING ON THE FOREIGN PATENT RIGHTS WHICH MAY BE INVOLVED.

REEL - C

151

A.T.I.

6476

ARR No. L5B17

NATIONAL ADVISORY COMMITTEE FOR AERONAUTICS

WARTIME REPORT

ORIGINALLY ISSUED

April 1945 as
Advance Restricted Report L5B17

WIND-TUNNEL INVESTIGATION OF A RECTANGULAR NACA 2212 AIRFOIL WITH SEMISPAN AILERONS AND WITH NONPERFORATED, BALANCED DOUBLE SPLIT FLAPS FOR USE AS AERODYNAMIC BRAKES

By Thomas A. Toll and Margaret F. Ivey

Langley Memorial Aeronautical Laboratory
Langley Field, Va.

NACA ARR No. L5B17

NATIONAL ADVISORY COMMITTEE FOR AERONAUTICS

ADVANCE RESTRICTED REPORT

WIND-TUNNEL INVESTIGATION OF A RECTANGULAR NACA 2212 AIRFOIL WITH SEMISPAN AILERONS AND WITH NONPERFORATED, BALANCED DOUBLE SPLIT FLAPS FOR USE AS AERODYNAMIC BRAKES

By Thomas A. Toll and Margaret F. Ivey

SUMMARY

Tests have been made in the Langley 7- by 10-foot tunnel to determine the applicability of nonperforated, balanced double split flaps for use as aerodynamic brakes. Information was desired on the braking power of the flaps as well as on the effectiveness and the stability of a conventional trailing-edge aileron located immediately behind the flaps.

A rectangular 10- by 60-inch wing model of NACA 2212 airfoil section was used for the tests. Results were obtained for flat-plate flaps with no wing cut-outs and for flaps having Clark Y sections with cut-outs made in the wing to simulate the space left open by the deflected flaps. The flap deflections, the chordwise location, and the gaps between the flaps and the airfoil contour were varied over wide ranges in order to determine the optimum configuration. In addition to the force tests, an investigation was made to determine any buffeting tendencies of the aileron. Silk tufts and a flexible torque rod were used for these tests.

The drag was only slightly lower for the model having airfoil-section flaps and wing cut-outs than for the model having flat-plate flaps and no cut-outs in the wing; for both arrangements the drag was higher than that obtained in previous tests of an NACA 23012 airfoil with full-span, 0.20-airfoil-chord, perforated double split flaps. The aileron effectiveness was low in either case, except when the flap gaps were equal to about 20 percent of the wing chord and when the noses of the flaps were at least 80 percent of the chord from the leading edge of the wing.

Although the entire model showed some tendency to shake, tufts indicated that the air flow over the aileron generally was smooth. Tests of the aileron attached to a flexible torque rod indicated almost no tendency for the aileron to shake; however, when the flap gaps were 15 percent of the wing chord or less, the aileron acted as though it were overbalanced and usually tended to float against the stops for either positive or negative deflections.

INTRODUCTION

The present investigation was made because certain unpublished data had indicated that satisfactory drag and lateral control characteristics had been obtained on an airplane with balanced double split flaps mounted ahead of a conventional aileron. Tests of balanced single split flaps on the lower surface of a wing had previously been made by the NACA (reference 1), and certain flap locations were found at which the aileron was as effective with flap deflected as with flap retracted. Tests of perforated double split flaps having no gaps between the flaps and the airfoil contour (references 2 to 5) showed that such flaps produced desirable lift, drag, and pitching-moment characteristics for use as dive brakes and that the drag increment increased as the flaps were moved forward on the wing. The tests reported in reference 2, however, showed that almost no effectiveness could be expected from an aileron located behind these flaps.

The present tests were made with a model configuration similar to that of references 2 and 4 but having two flaps, similar to the flap of reference 1, symmetrically disposed above and below the wing. It was desired to determine if there were any flap locations at which sufficient lateral control as well as satisfactory drag characteristics could be obtained simultaneously.

APPARATUS AND TESTS

Model

The wing model was built of mahogany to the NACA 2212 profile. The model was of rectangular plan form; the span

was 60 inches and the chord, 10 inches. Semispan ailerons having chords equal to 18.5 percent of the wing chord (0.185c) were provided. The ailerons were not balanced and had small gaps at their leading edges.

Two sets of flaps were used with the model. Both sets were full span, were nonperforated, and had chords of 2 inches. One set was made of flat steel plate $\left(\frac{1}{16}\text{-in. thick}\right)$ and had rounded leading edges. Each flap of this set was attached to the wing by eight fittings along the span. The fittings were adjustable to allow variations of flap deflections, chordwise locations, and gaps between the flaps and the wing. The wing had no cut-outs to simulate the space left by the flaps when deflected. Photographs of the model mounted in the tunnel are given as figures 1 and 2. The second set of flaps was constructed of steel plate and wood to the Clark Y section (fig. 3). Cut-outs in the wing were made to simulate the space left by the flaps when deflected. Each flap was attached to the wing by six fittings, which rested on narrow bridges left across the wing cut-outs.

The dimensions of the model and the flap locations and deflections tested are given in figures 4 and 5.

Tests

The dynamic pressure maintained for all tests was 16.37 pounds per square foot, which corresponds to a velocity of about 80 miles per hour under standard sea-level conditions and to a test Reynolds number of 609,000 based on the chord of the model wing (10 in.). The effective Reynolds number, based on a turbulence factor of 1.6 for the Langley 7- by 10-foot tunnel, was about 975,000.

The tests consisted principally of the determination of the lift, drag, and pitching-moment characteristics of the model with the ailerons neutral and of the rolling- and yawing-moment characteristics of the model with the right aileron at various fixed deflections. A few tests were made to determine the aileron hinge-moment coefficients and to investigate the flow conditions in the vicinity of the aileron.

Tests of the model with no wing cut-outs and with flat-plate flaps were made with the flaps at a number of chordwise locations, gaps, and deflections. Only a few configurations of the model with airfoil-section flaps and with wing cut-outs were tested. These tests were made principally to check the validity of the assumption that the wing cut-outs and the flap section would have little effect on the results when the flaps are at high deflections.

RESULTS AND DISCUSSION

Symbols

In the presentation of the results, the following symbols are used:

C_L	lift coefficient (L/qS)
C_D	drag coefficient (D/qS)
$C_{m_{c/4}}$	pitching-moment coefficient about quarter-chord point of airfoil $\left(\frac{M_{c/4}}{qSc}\right)$
C_h	aileron hinge-moment coefficient $\left(H/qb_a c_a^2\right)$
C_l'	rolling-moment coefficient (L'/qSb)
C_n'	yawing-moment coefficient (N'/qSb)

where

L	lift
D	drag
H	aileron hinge moment
$M_{c/4}$	pitching moment about quarter-chord point of airfoil
L'	rolling moment about wind axis in plane of symmetry of model

N'	yawing moment about wind axis in plane of symmetry of model
q	dynamic pressure of free air stream $\left(\frac{\rho V^2}{2}\right)$
ρ	density
V	velocity
c	wing chord
c_a	aileron chord
S	wing area
b	wing span
b_a	span of aileron
α	angle of attack
δ_a	aileron deflection
δ_{f_U}	upper-surface split-flap deflection measured from wing chord line
δ_{f_L}	lower-surface split-flap deflection measured from wing chord line

Gap is defined as the distance, measured perpendicular to the wing chord line, between the true airfoil contour and the portion of the flap nearest the airfoil contour. (See figs. 4 and 5.)

Chordwise location is defined as the distance, measured parallel to the wing chord line, between the wing leading edge and the tangent - perpendicular to the wing chord line - to the portion of the flap nearest the airfoil contour. (See figs. 4 and 5.)

Aileron effectiveness is defined as the increment of rolling-moment coefficient between curves corresponding to two fixed aileron deflections.

Corrections

No corrections were applied for the effects of support-strut interference. The standard jet-boundary

corrections, which were applied to all the force-test data, are:

$$\Delta\alpha = \delta\frac{S}{C}C_L\ 57.3$$

$$\Delta C_D = \delta\frac{S}{C}C_L^2$$

where $\Delta\alpha$ is in degrees, δ is the jet-boundary correction factor, and C is the cross-sectional area of the jet (69.59 sq ft). A value of $\delta = 0.112$ for the closed-throat wind tunnel was used in correcting the results. No corrections were applied to the pitching-, yawing-, rolling-, or hinge-moment coefficients; these corrections are all small because of the relatively small size of the model.

Wing without Flaps

Tests were made of the model without flaps in order to provide a basis upon which to compare the tests of the model with flaps. The results of these tests are given in figures 6 to 8. The almost linear variation of lift coefficient with angle of attack (fig. 6), the large and almost constant increment of rolling-moment coefficient between aileron deflections of ±20° (fig. 7), and the approximately constant negative slope of the hinge-moment curves (fig. 8) should be noted.

Wing with Flat-Plate Flaps

The model was tested with two symmetrically located flat-plate flaps at a number of chordwise locations, gaps, and deflections. The results of the tests are given in figures 9 to 20. The effect of flap deflection (flaps located at 0.80c and with 0.05c gaps) is given in figure 9. A comparison of this figure with figure 6 indicates that, at zero angle of attack, increments of drag coefficient of 0.232 and 0.468 are produced by the flaps when deflected 30° and 60°, respectively. Comparable values of the drag increment caused by full-span, 0.20c, perforated double split flaps at the same chordwise

location on an NACA 23012 airfoil (fig. 3 of reference 2) are 0.14 and 0.33. The irregularities in the curves of C_L against α for the model with flaps deflected (fig. 9) are of interest. The effectiveness of the ailerons is very low - at times, even negative - for this configuration (fig. 10).

When the flaps are deflected 30°, the irregularities in the curve of C_L against α are less pronounced when the gaps are 0.10c (fig. 11) than when the gaps are 0.05c (fig. 9). The aileron effectiveness is greater when the gaps are 0.10c (fig. 12) than when the gaps are 0.05c (fig. 10). Increasing the flap deflection to 60° results in large irregularities in the curves of C_L against α (fig. 13) as well as in reductions in the lift-curve slopes, particularly when the flaps are located far forward. The aileron effectiveness (fig. 14) is generally lower and more irregular when flaps are deflected 60° than when flaps are deflected 30° (fig. 12). Tests were made with aileron deflections of ±10° as well as 0° and ±20° for the condition of the flaps located at 0.80c (fig. 14(c)), in order to determine if greater effectiveness might be obtained at the smaller aileron deflections. The effectiveness seems to increase almost linearly with deflection for low angles of attack but is about the same for $\delta_a = \pm 10°$ as for $\delta_a = \pm 20°$ at high angles of attack.

The characteristics of the model with the flaps deflected 60° and with gaps of 0.15c are given in figures 15 and 16. The irregularities in the lift curves increase in magnitude as the flaps are moved forward (fig. 15). The aileron effectiveness decreases as the flaps are moved forward (fig. 16).

With the flaps located at 0.80c and with gaps of 0.20c, tests were made with the flaps deflected 60°, 90°, and 120° (figs. 17 and 18). The lift curves for the conditions of flaps deflected 60° and 120° are characterized by flat regions near zero angle of attack (fig. 17). When the flaps were deflected 90°, an irregularity occurred, which was similar to those noted previously. The maximum values of the lift-curve slopes for these conditions are only about one-half the value of the lift-curve slope for the model without flaps (fig. 6). The aileron effectiveness is relatively high

(about 80 percent of the effectiveness when no flaps are attached) and does not seem to be appreciably affected by the flap deflection (fig. 18).

Tests were made with flap chordwise locations of 0.90c, gaps of 0.20c, and deflections of 60° and 120°. The results are given in figures 19 and 20. The condition of flaps deflected 60° seems to be the most favorable of all the configurations that have been discussed. The lift curve (fig. 19) is almost linear and the value of its slope for angles of attack greater than 2° is about 80 percent of the value of the lift-curve slope of the model without flaps (fig. 6). The ailerons are as effective as when no flaps are attached.

Tests were made with one flap located at 0.80c, with a 0.10c gap, and with a deflection of 60° (figs. 21 and 22). For the negative angle-of-attack range with the flap placed below the airfoil and for the positive angle-of-attack range with the flap placed above the airfoil, the effectiveness of the aileron for ±20° deflection is about the same as the effectiveness when no flaps are attached. When the flap is below the airfoil, the effectiveness of the aileron deflected 20° decreases as the angle of attack is increased above -2° (fig. 22(a)). When the flap is above the airfoil, the effectiveness of the aileron deflected -20° decreases as the angle of attack is decreased below -2° (fig. 22(b)).

Wing with Airfoil-Section Flaps

The results of tests of the model with Clark Y airfoil-section flaps are given in figures 23 to 37. The lift, drag, and pitching-moment characteristics of the model with flaps deflected 30° and at chordwise locations of 0.60c and 0.70c are given in figure 23(a) for flap gaps of 0.05c and in figure 23(b) for flap gaps of 0.10c. A comparison of the curves for the 0.70c location of figure 23(b) with the corresponding curves of figure 11 reveals that the airfoil-section flaps and wing cut-outs result in slight decreases in the drag coefficients. A similar effect through most of the angle-of-attack range may be noted by comparing figures 27, 29, and 31 with figures 13, 15, and 17, respectively. Part of the reduction in drag coefficient is probably a result of the fact that fewer fittings were used to attach the airfoil-section flaps to the wing than were

used to attach the flat-plate flaps to the wing. The aileron effectiveness generally is slightly higher for the model having airfoil-section flaps and wing cut-outs than for the model having flat-plate flaps and no cut-outs in the wing; this fact can be noted by comparing figures 28, 30, and 32 with figures 14(a) and 14(b), 16(b) and 16(c), and 18(a), respectively.

The variation of the rolling-moment coefficient with aileron deflection was determined for the model with the flaps located at 0.70c and with gaps of 0.15c and 0.20c (fig. 33). At an angle of attack of 0° the rolling-moment coefficient varied almost linearly with aileron deflection, but at an angle of attack of 12.1° the variation with negative deflections was irregular when the gaps were 0.15c.

Aileron hinge moments were measured for a number of model configurations and are presented in figures 34 and 35. When the flap gaps were 0.15c or less, the aileron seemed to be overbalanced and usually tended to float against the stops for either positive or negative deflections. With the flaps located at 0.70c or at 0.80c, the overbalance was eliminated by increasing the gaps to 0.20c. At an angle of attack of 0° and at small aileron deflections, the slope $\partial C_h/\partial \delta_a$ was still considerably less negative, however, than when no flaps were attached to the model (fig. 8).

Because the model had a tendency to shake when the flaps were deflected 60° or more, an investigation was made to determine if this shake were accompanied by a buffeting tendency of the aileron. No such tendency was noted when the aileron was restrained only by the flexible torque rod used for the hinge-moment measurements. The investigation was extended by observing silk tufts mounted from masts attached to the aileron at its midspan, midchord location. The directions and the stability of the various tufts are indicated in figure 36 for several model configurations. The tufts on and near the surfaces of the aileron were almost invariably smooth and were pointed in the downstream direction. Aileron buffeting therefore does not seem to be a serious problem for an airplane with balanced double split flaps.

A summary of the effects of gap and of chordwise location of the two sets of flaps (each set at deflections of 60°) on the aileron effectiveness relative to

that of the plain wing and on the drag coefficients is presented in figure 37. The aileron effectiveness increases as the gaps are increased and as the flaps are moved rearward. The drag increases as the gaps are increased and as the flaps are moved forward. The variation in drag is probably caused by the increased depth of the wake as the flaps are moved forward while constant gaps are maintained between the flaps and the surfaces of the wing and also by the higher local velocities occurring at the forward portions of the wing. Reference 5 showed that the increment of drag caused by perforated double split flaps was more than doubled when the flaps were moved from the wing trailing edge to the 0.30c location. From the results of the tests reported herein, however, the 0.30c location would be expected to result in little or no effectiveness of ailerons located back of the flaps, even though the gaps were large. Because the reduction in drag as the flaps are moved rearward of the 0.60c location is not very great and because the rearward flap locations result in improvements in the other wing and aileron characteristics, it seems desirable to locate balanced double split flaps at about 0.30c or farther rearward. Gaps of about 0.20c are necessary to obtain satisfactory wing lift, aileron-effectiveness, and aileron hinge-moment characteristics.

CONCLUSIONS

From the results of tests of full-span, nonperforated, balanced split flaps on a rectangular NACA 2212 airfoil, the following conclusions may be drawn:

1. The effectiveness of a conventional aileron behind balanced double split flaps was generally low but increased as the flaps were moved rearward and as the gaps between the flaps and the airfoil surfaces were increased.

2. The drag of the model increased as the flaps were moved forward and as the flap gaps were increased.

3. There was usually an irregularity in the curve of lift coefficient against angle of attack for the model with balanced double split flaps deflected. The magnitude of the irregularity increased as the flaps

were moved forward, as the flap gaps were decreased, and as the flap deflections approached 90°.

4. The slope of the curve of lift coefficient against angle of attack generally decreased as the flaps were moved forward and as the flap gaps were increased.

5. An aileron back of a balanced single split flap with a small flap gap may be as effective through a large part of the angle-of-attack range as an aileron on a wing having no flaps.

6. The effectiveness of the aileron on the model having airfoil-section flaps and wing cut-outs was generally slightly higher than the effectiveness of the aileron on the model having flat-plate flaps and no wing cut-outs.

7. The drag of the model having airfoil-section flaps and wing cut-outs was generally slightly lower than the drag of the model having flat-plate flaps and no wing cut-outs.

8. Although the model with balanced double split flaps showed some tendency to shake, the aileron was usually steady and the air flow was smooth on and near the surface of the aileron.

9. Plain ailerons back of balanced double split flaps acted as though they were highly overbalanced when the flap gaps were 15 percent of the wing chord or less.

10. From a consideration of lift, drag, aileron-effectiveness, and aileron hinge-moment characteristics, a satisfactory practical configuration probably could be obtained with balanced double split flaps located at 80 percent of the wing chord and with flap gaps of 20 percent of the wing chord.

11. The drag of this model was higher than the drag of an NACA 23012 airfoil with full-span, 0.20-airfoil-chord, perforated double split flaps at the same chordwise location.

Langley Memorial Aeronautical Laboratory
National Advisory Committee for Aeronautics
Langley Field, Va.

REFERENCES

1. Rogallo, F. M., and Lowry, John G.: Wind-Tunnel Investigation of a Plain Aileron and a Balanced Aileron on a Tapered Wing with Full-Span Duplex Flaps. NACA ARR, July 1942.

2. Purser, Paul E., and Turner, Thomas R.: Wind-Tunnel Investigation of Perforated Split Flaps for Use as Dive Brakes on a Rectangular NACA 23012 Airfoil. NACA ACR, July 1941.

3. Purser, Paul E., and Turner, Thomas R.: Wind-Tunnel Investigation of Perforated Split Flaps for Use as Dive Brakes on a Tapered NACA 23012 Airfoil. NACA ARR, Nov. 1941.

4. Purser, Paul E., and Turner, Thomas R.: Aerodynamic Characteristics and Flap Loads of Perforated Double Split Flaps on a Rectangular NACA 23012 Airfoil. NACA ARR, Jan. 1943.

5. Blenkush, Philip G., Hermes, Raymond F., and Landis, Merle A.: Effect of Dive Brakes on Airfoil and Airplane Characteristics. Jour. Aero. Sci., vol. 11, no. 3, July 1944, pp. 254-260.

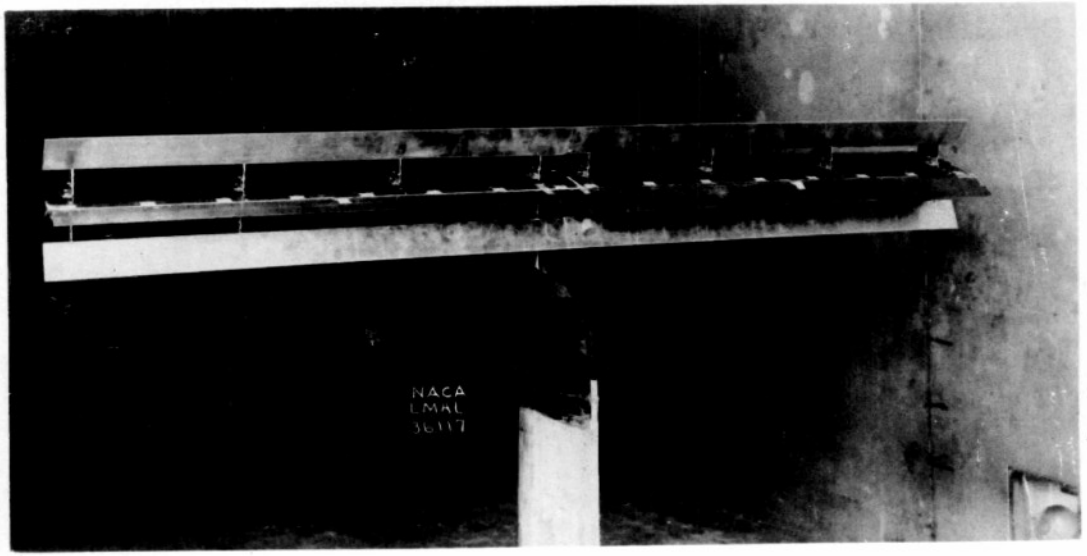

Figure 1.- Three-quarter rear view of the 10- by 60-inch rectangular NACA 2212 airfoil with full-span, nonperforated, balanced double split flaps of 20-percent airfoil chord mounted in the Langley 7- by 10-foot tunnel. Flat-plate flaps deflected 60° and located at 0.60c with gaps of 0.15c; right aileron deflected.

(13)

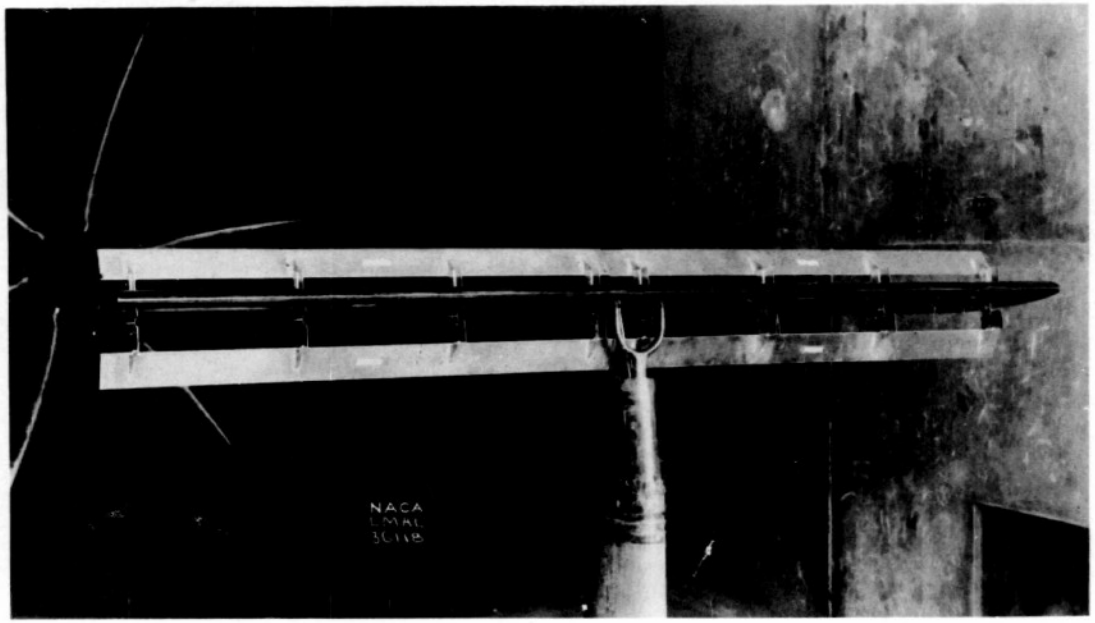

Figure 2.- Three-quarter front view of the 10- by 60-inch rectangular NACA 2212 airfoil with full-span, nonperforated, balanced double split flaps of 20-percent airfoil chord mounted in the Langley 7- by 10-foot tunnel. Flat-plate flaps deflected 60° and located at 0.60c with gaps of 0.15c; right aileron deflected.

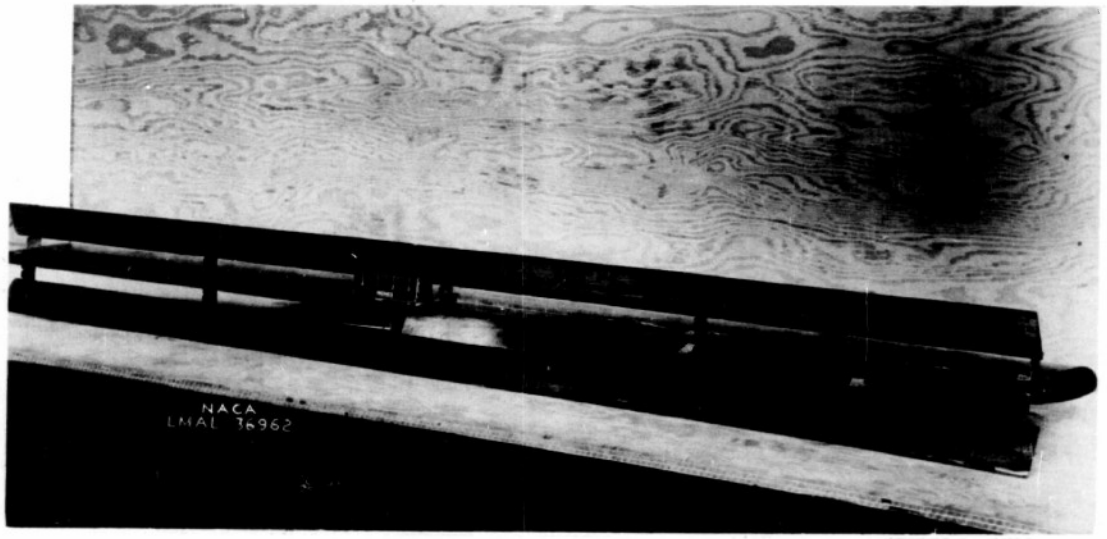

Figure 3.- Three-quarter rear view of the 10- by 60-inch rectangular NACA 2212 airfoil with full-span, nonperforated, balanced double split flaps of 20-percent airfoil chord. Airfoil-section flaps deflected 60° and located at 0.70c with gaps of 0.10c; right aileron deflected.

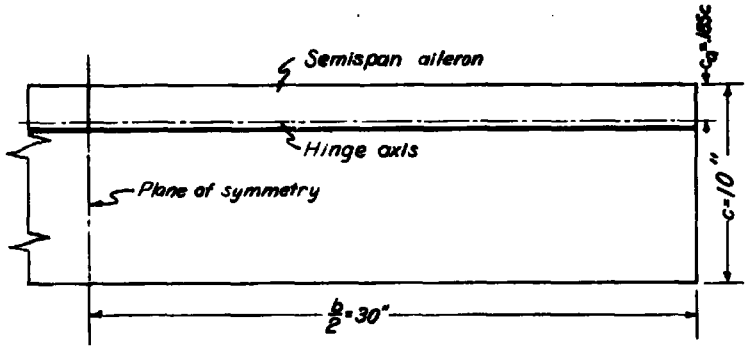

(a) Plan form of wing.

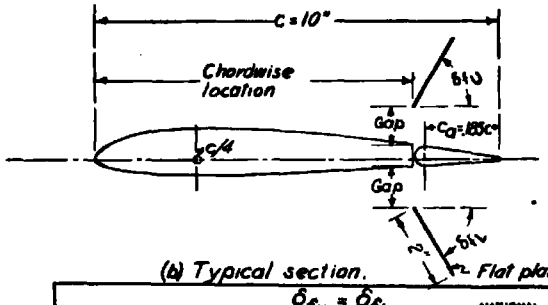

(b) Typical section.

$\delta_{fU} = \delta_{fL}$ (deg)

NATIONAL ADVISORY COMMITTEE FOR AERONAUTICS

Gap \ Chordwise location	0.60c	0.70c	0.80c	0.90c
0.05c			30 and 60	
.10c	60	30 and 60	30 and 60	
.15c	60	60	60	60
.20c			60,90, and 120	60 and 120

(c) Flap deflections for various chordwise locations and gaps.

Figure 4.- Dimensions and flap configurations of the model with balanced double split flaps having flat-plate sections. Wing airfoil section, NACA 2212.

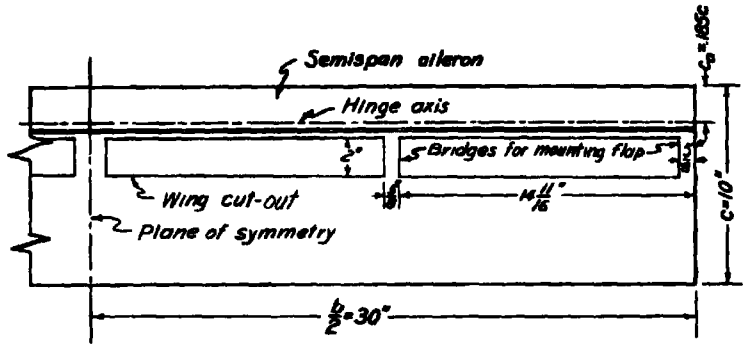

(a) Plan form of wing.

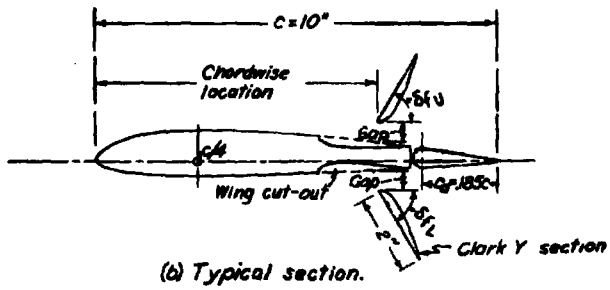

(b) Typical section.

Gap \ Chordwise location	$\delta_{fU} = \delta_{fL}$ (deg) 0.60c	0.70c	0.80c
0.05c	30 and 60	30 and 60	
.10c	30 and 60	30 and 60	
.15c	60	60	60
.20c		60	60

NATIONAL ADVISORY COMMITTEE FOR AERONAUTICS

(c) Flap deflections for various chordwise locations and gaps.

Figure 5.- Dimensions and flap configurations of the model with balanced double split flaps having Clark Y sections. Wing airfoil section, NACA 2212.

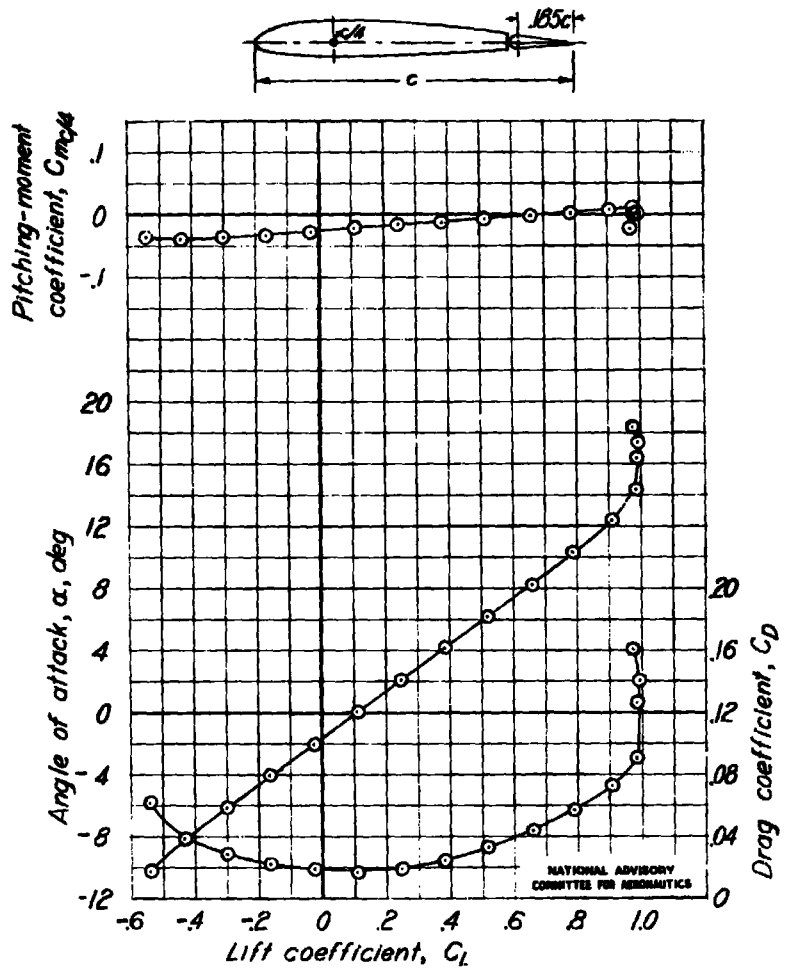

Figure 6.- Lift, drag, and pitching-moment characteristics of the NACA 2212 wing model. No flaps; δ_a, 0°.

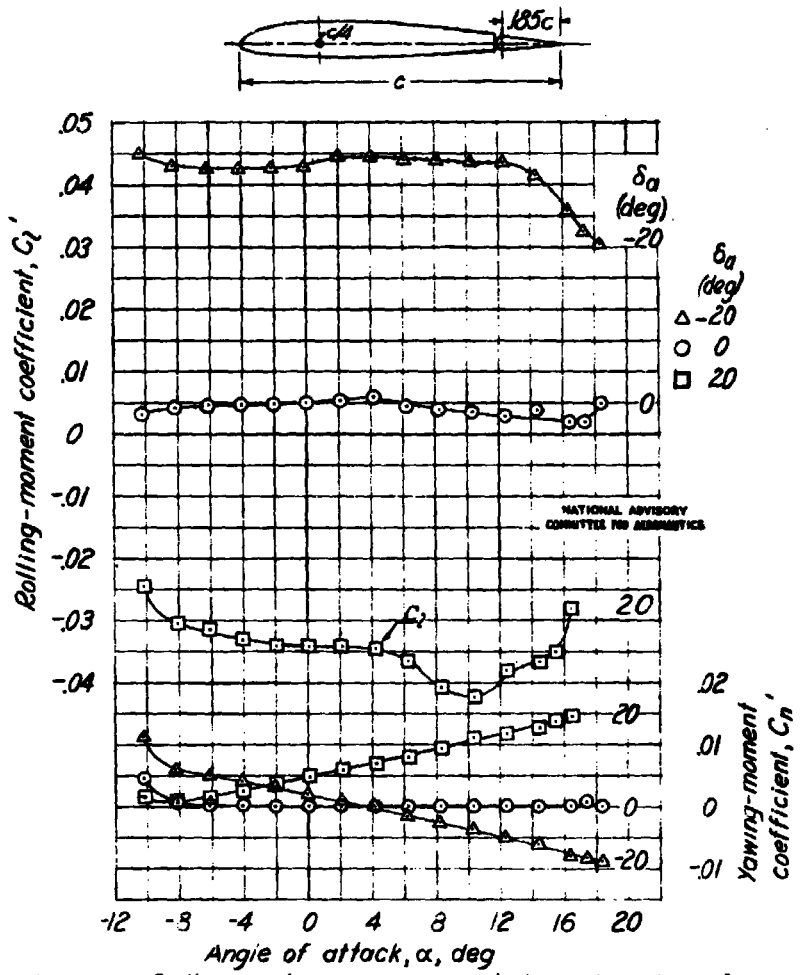

Figure 7.- Rolling- and yawing-moment characteristics of the right semispan aileron on the NACA 2212 wing model. No flaps.

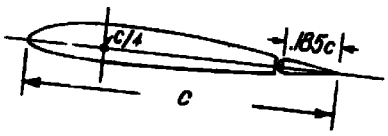

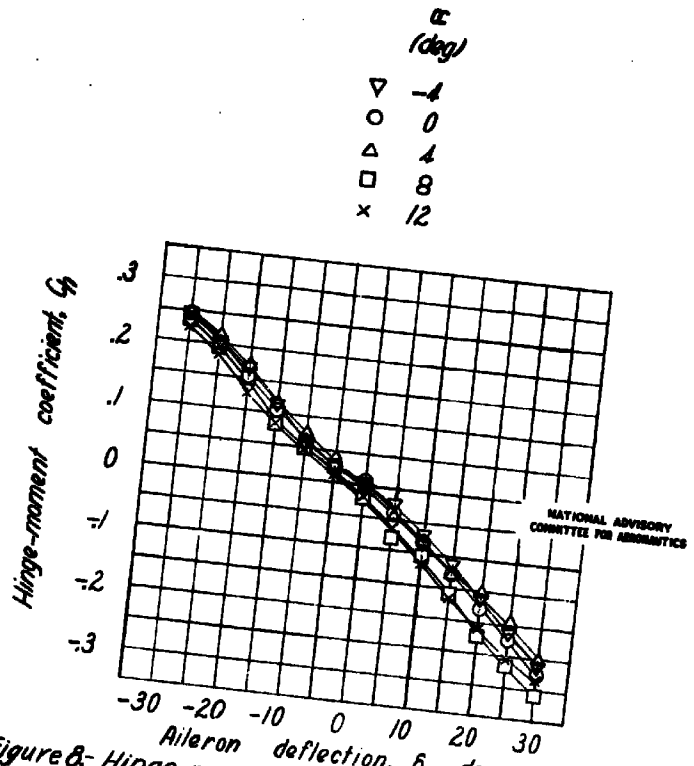

Figure 8.- Hinge-moment characteristics of the right semispan aileron on the NACA 2212 wing model. No flaps.

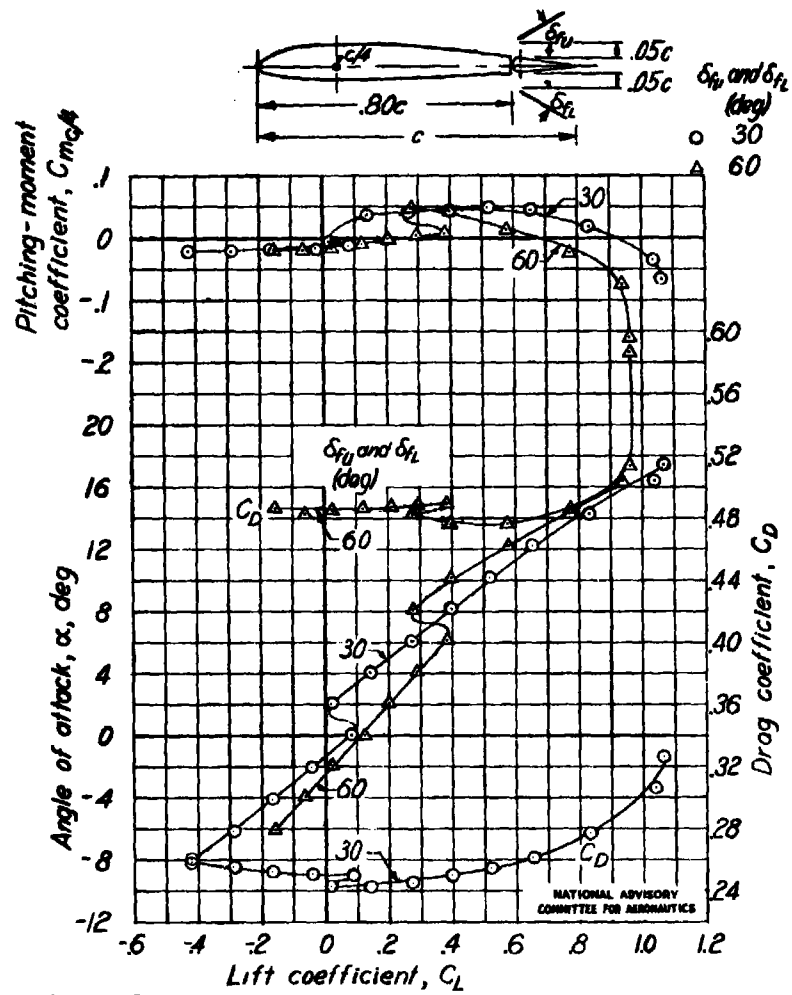

Figure 9.-Lift, drag, and pitching-moment characteristics of the NACA 2212 wing model equipped with balanced double split flaps having flat-plate sections. Chordwise location, 0.80c; gaps, 0.05c; δ_a, 0°.

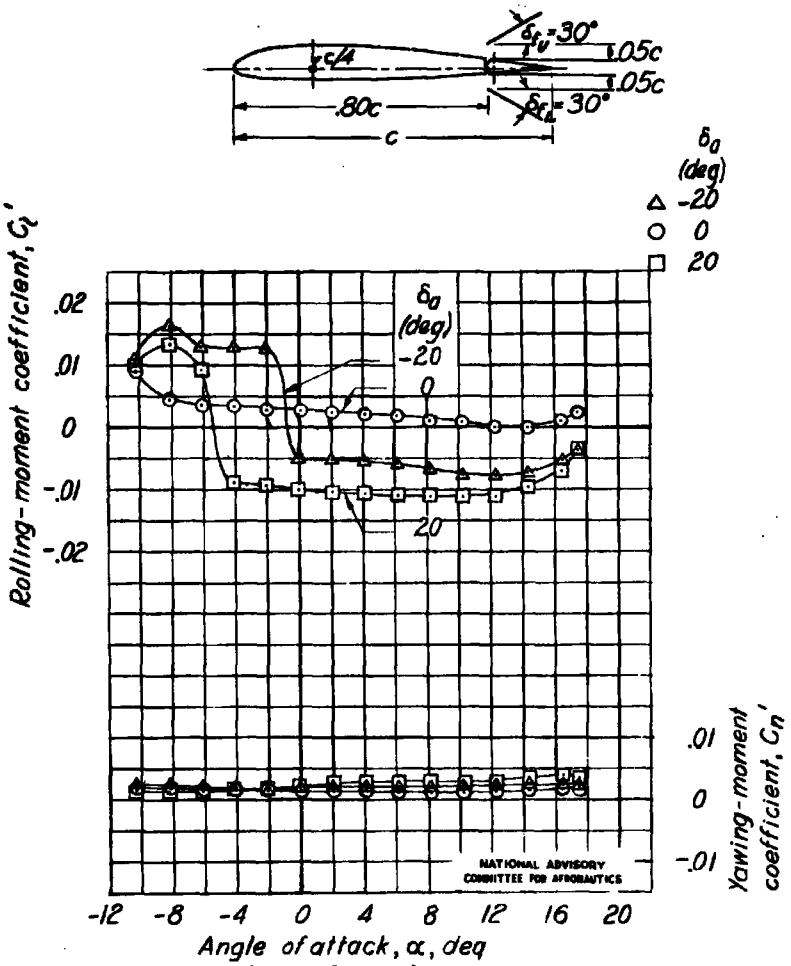

(a) δ_{f_U} and δ_{f_L}, 30°.

Figure 10.- Rolling- and yawing-moment characteristics of the right semispan aileron on the NACA 2212 wing model equipped with balanced double split flaps having flat-plate sections. Chordwise location, 0.80c; gaps, 0.05c.

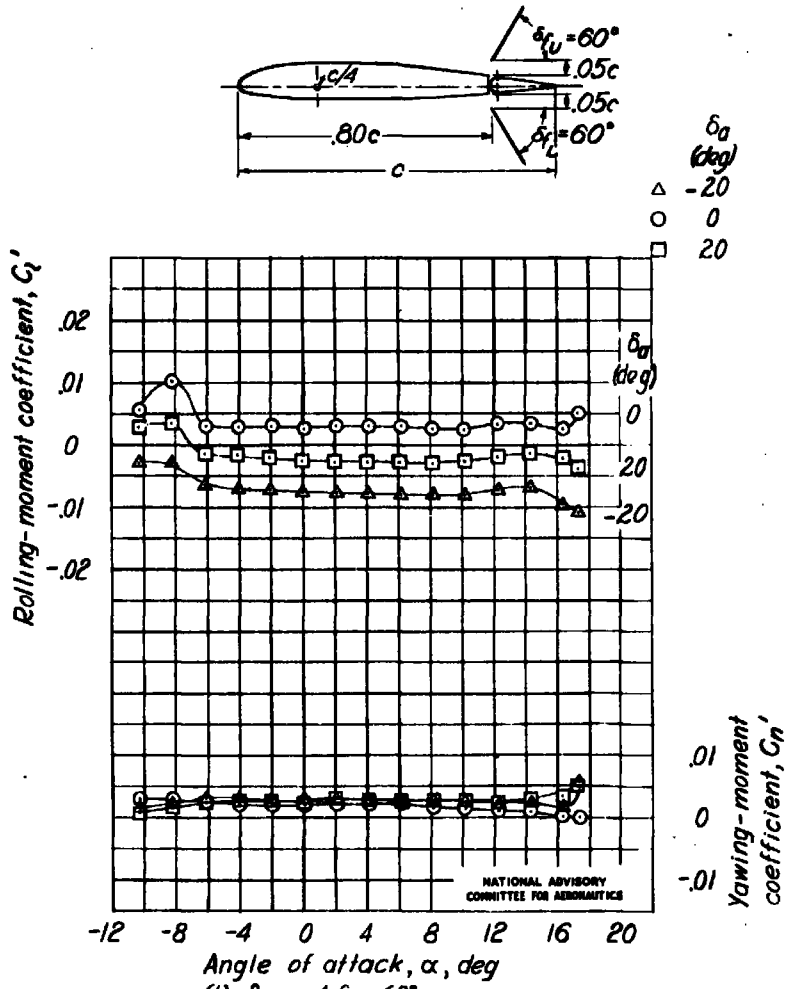

(b) δ_{f_U} and δ_{f_L}, 60°.

Figure 10-Concluded.

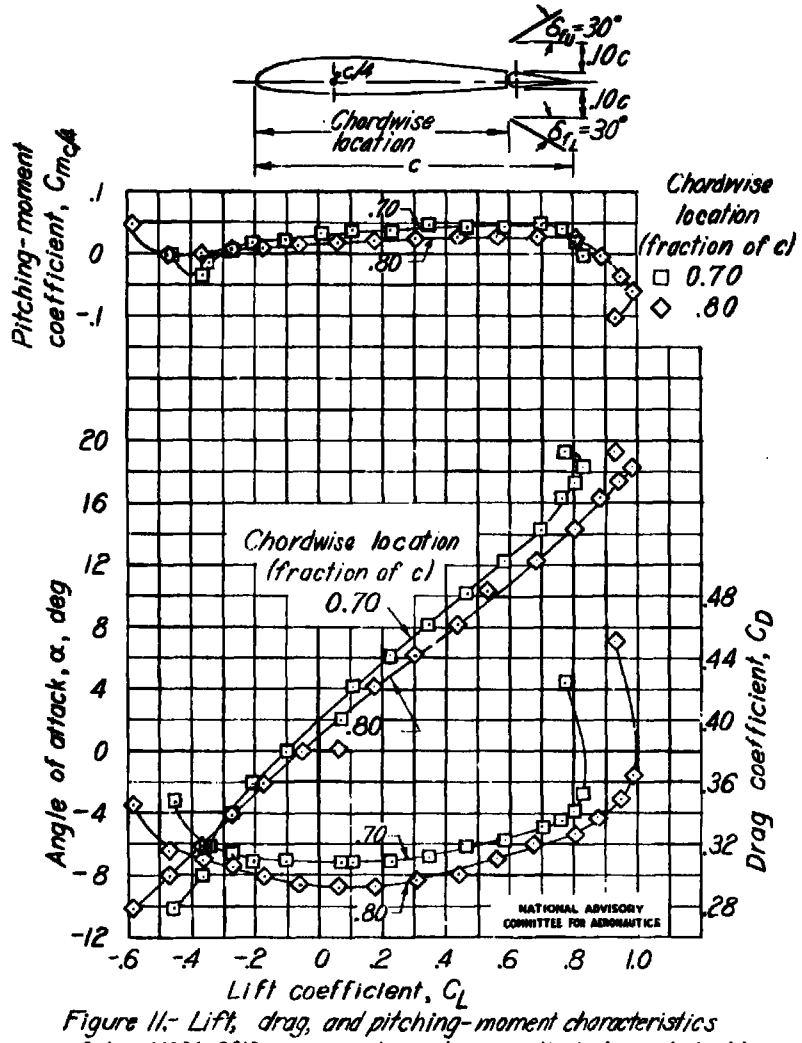

Figure 11.- Lift, drag, and pitching-moment characteristics of the NACA 2212 wing model equipped with balanced double split flaps having flat-plate sections. Gaps, 0.10c, δ_a, 0°; δ_{fU} and δ_{fL}, 30°.

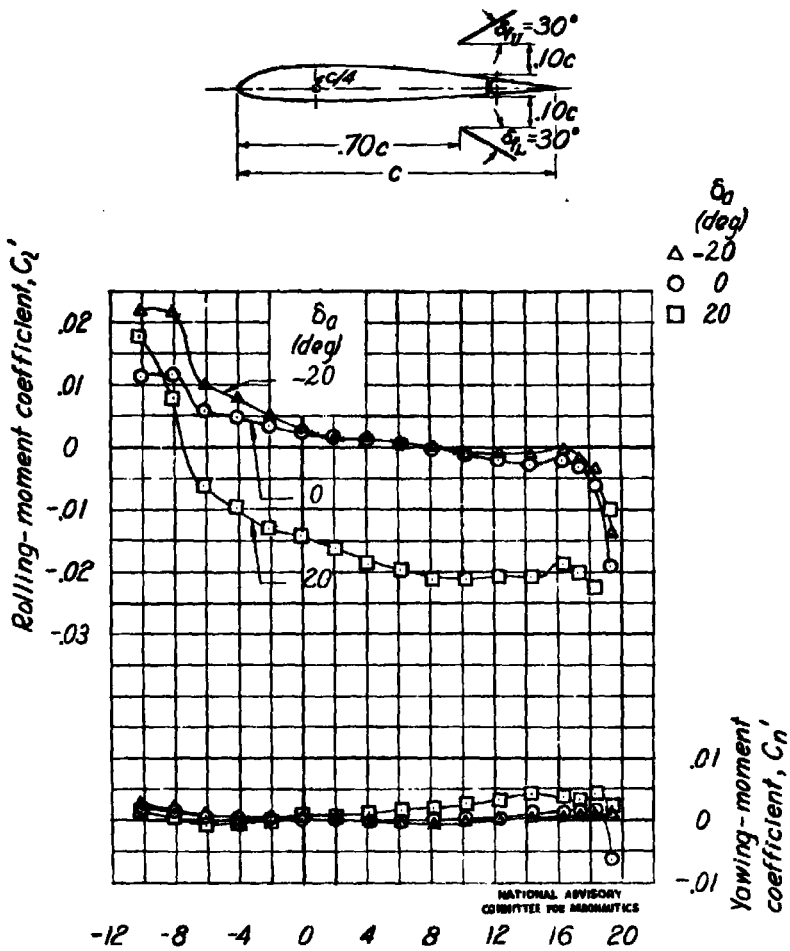

(a)Chordwise location, 0.70c.

Figure 12.- Rolling- and yawing-moment characteristics of the right semispan aileron on the NACA 2212 wing model equipped with balanced double split flaps having flat-plate sections. Gaps, 0.10c; δ_{n_U} and δ_{n_L}, 30°.

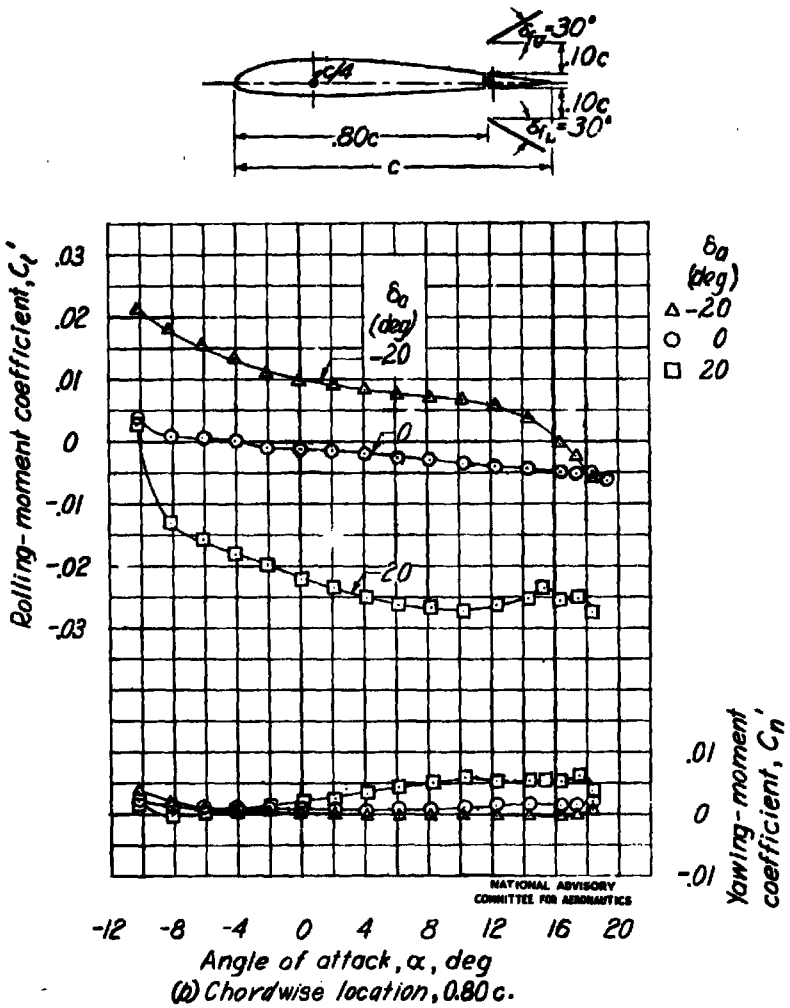

(b) Chordwise location, 0.80 c.

Figure 12.- Concluded.

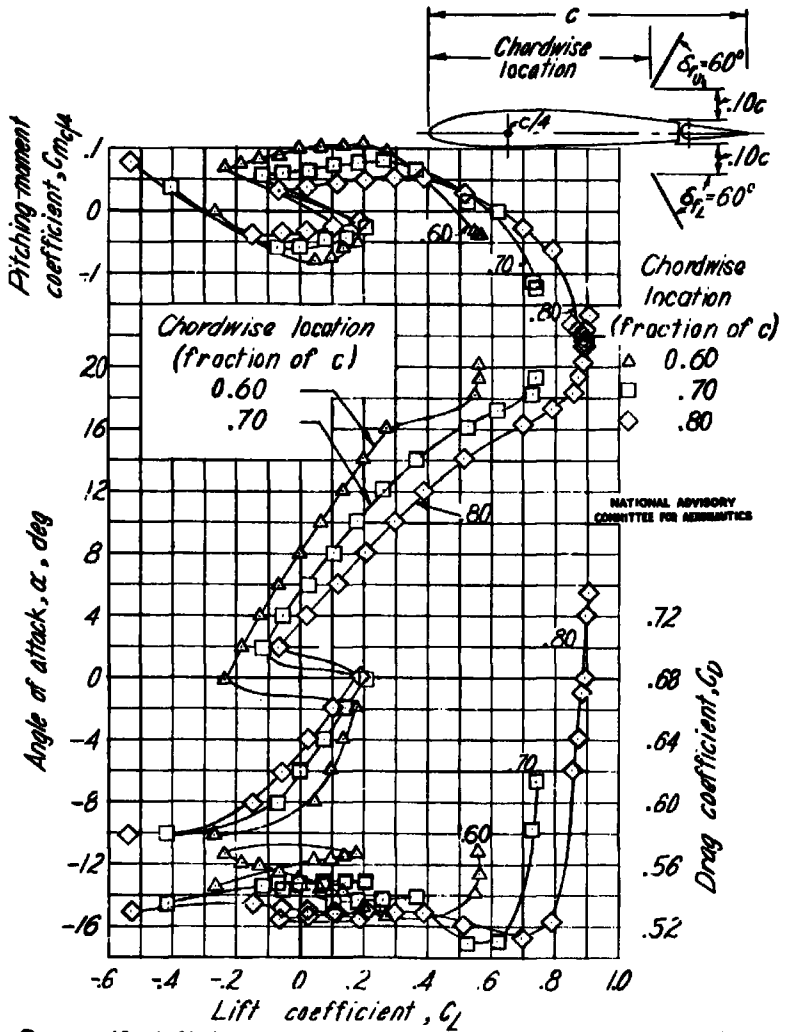

Figure 13.- Lift, drag, and pitching-moment characteristics of the NACA 2212 wing model equipped with balanced double split flaps having flat-plate sections. Gaps, 0.10c; δ_a, 0°; δ_{f_U} and δ_{f_L}, 60°.

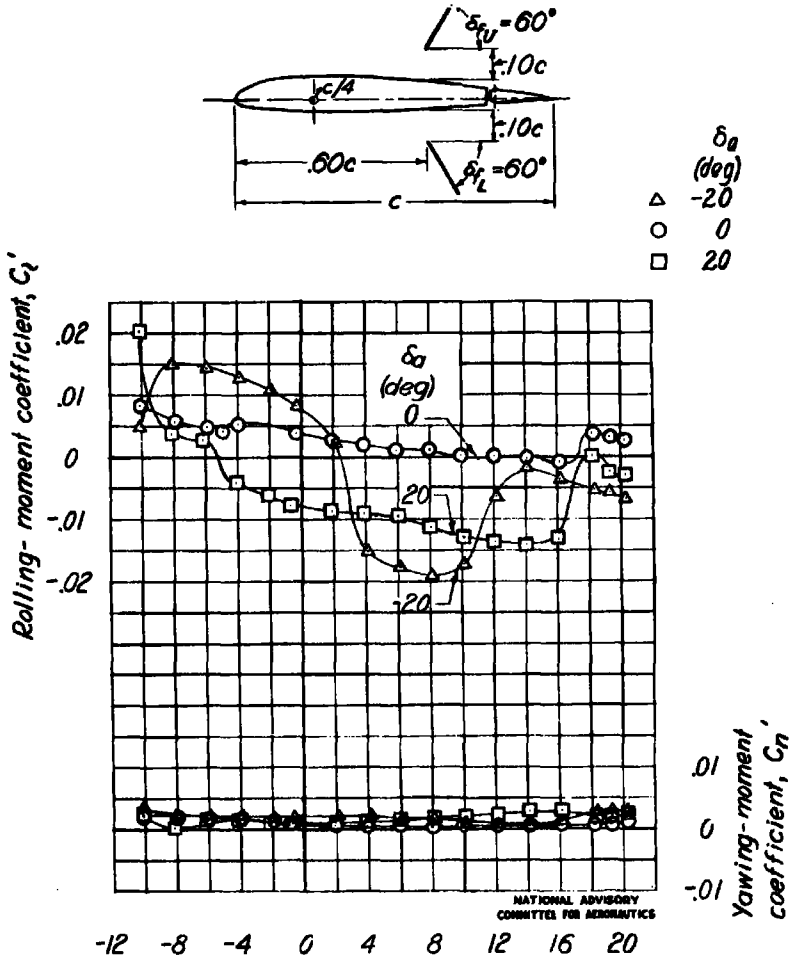

(a) Chordwise location, 0.60c.

Figure 14.- Rolling- and yawing-moment characteristics of the right semispan aileron on the NACA 2212 wing model equipped with balanced double split flaps having flat-plate sections Gaps, 0.10c; δ_{f_U} and δ_{f_L}, 60°.

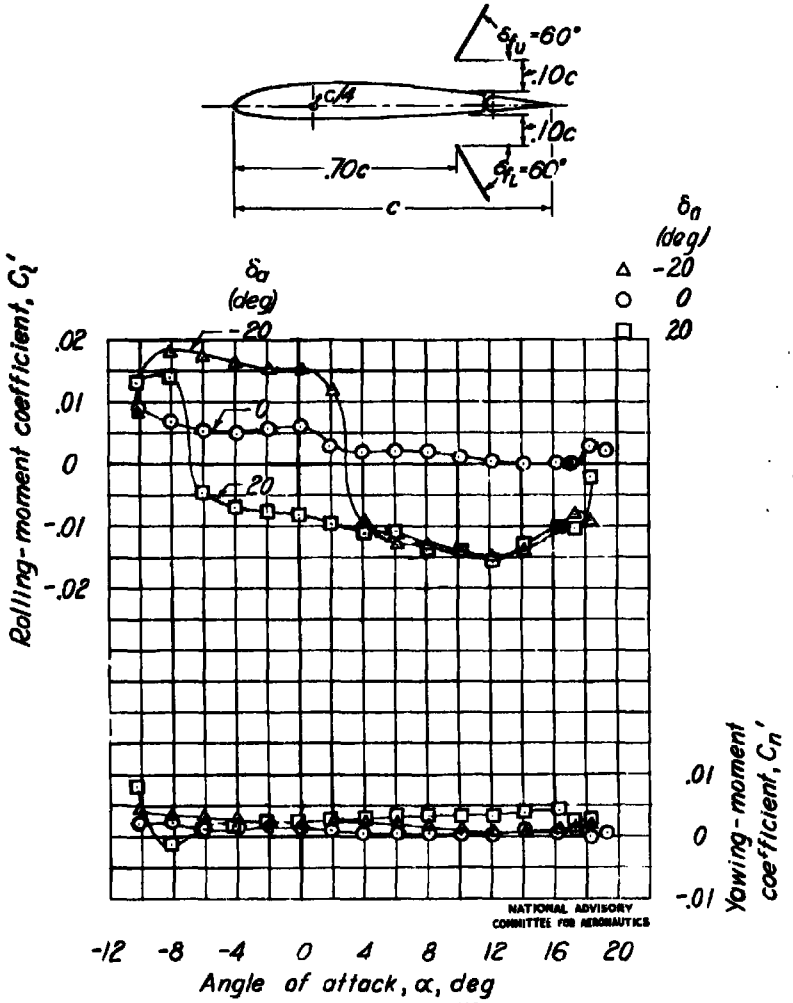

(b) Chordwise location, 0.70c.

Figure 14.-Continued.

(23)

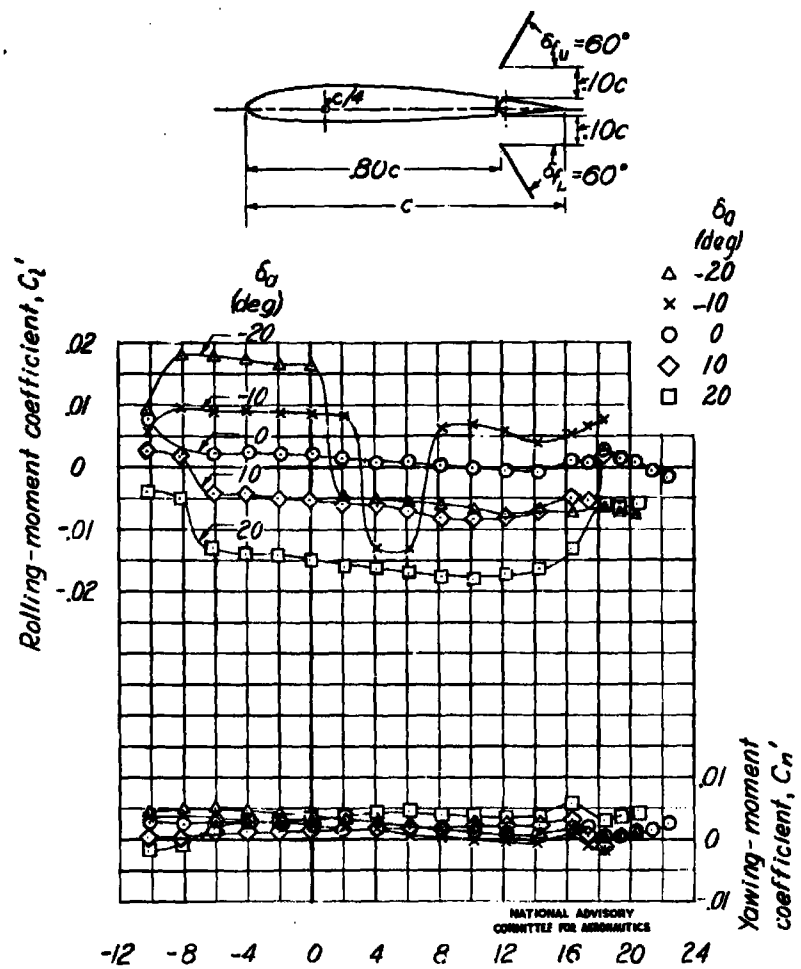

(c) Chordwise location, 0.80c.

Figure 14.- Concluded.

Fig. 15

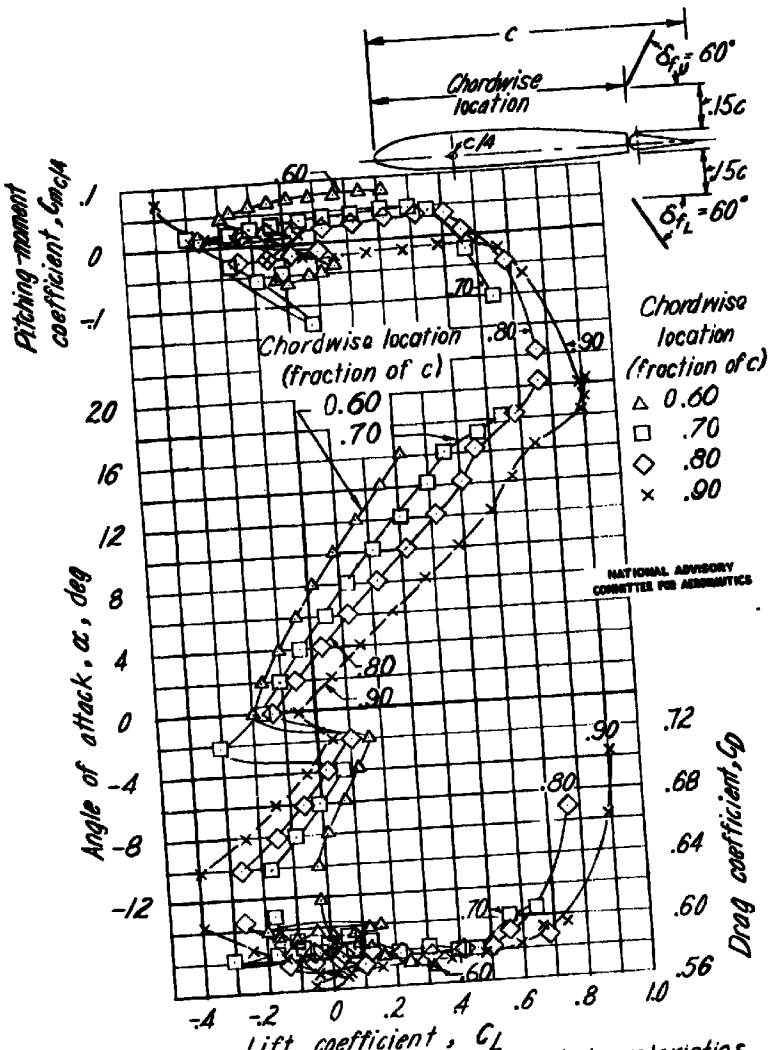

Figure 15.-Lift, drag, and pitching-moment characteristics of the NACA 2212 wing model equipped with balanced double split flaps having flat-plate sections. Gaps, 0.15c; δ_a, 0°; δ_{f_U} and δ_{f_L}, 60°.

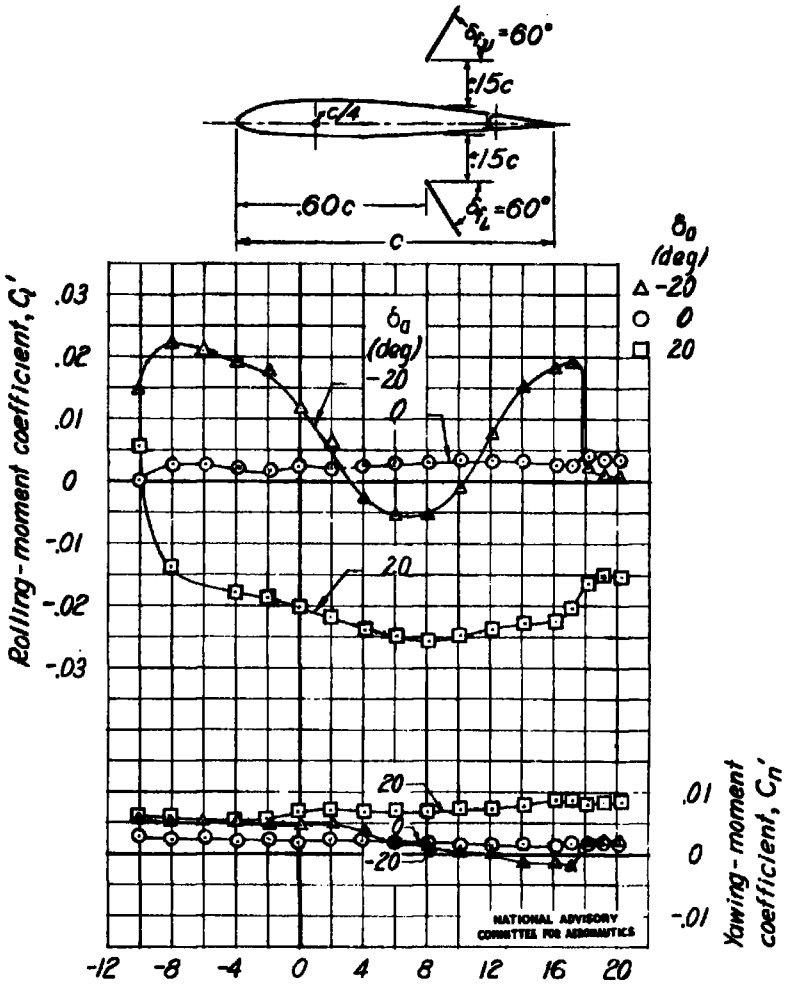

(a) Chordwise location, 0.60c.

Figure 16.- Rolling- and yawing-moment characteristics of the right semispan aileron on the NACA 2212 wing model equipped with balanced double split flaps having flat-plate sections. Gaps, 0.15c, δ_{f_U} and δ_{f_L}, 60°.

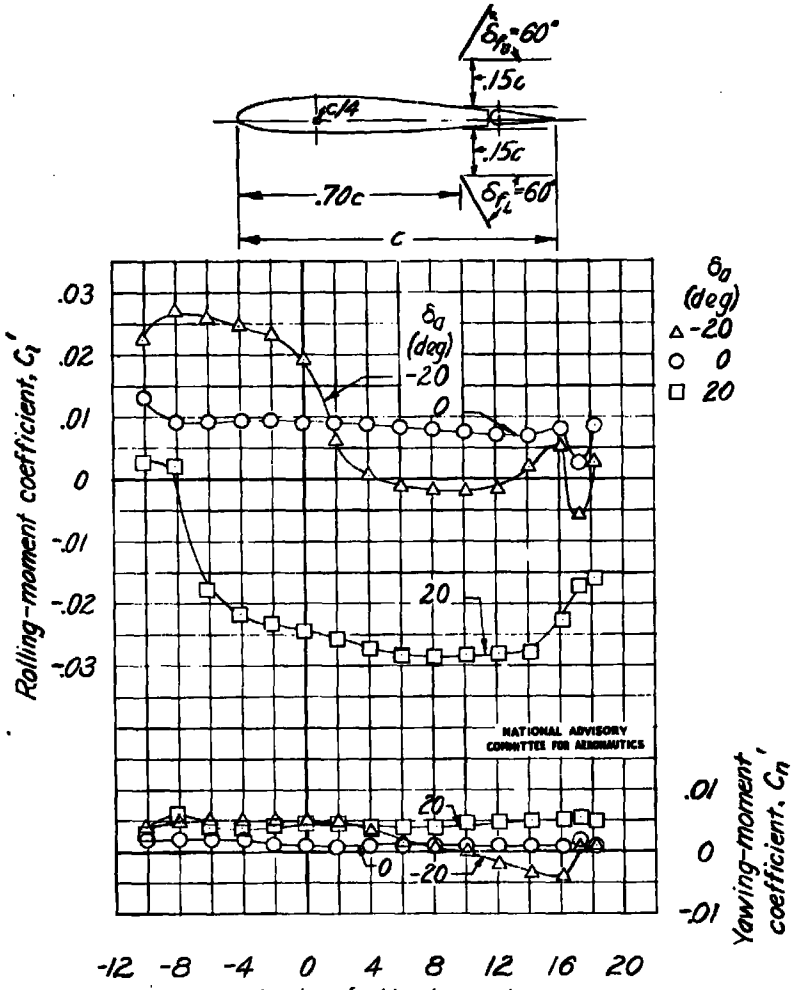

(b) Chordwise location, 0.70c.

Figure 16.- Continued.

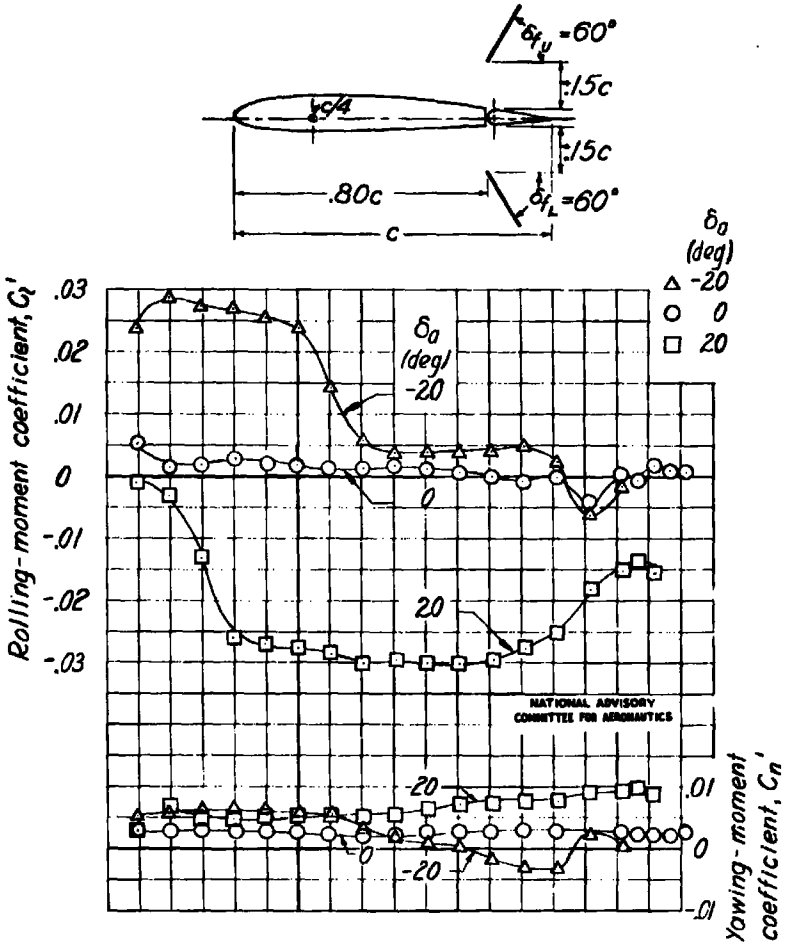

(c) Chordwise location, 0.80c.

Figure 16.- Continued.

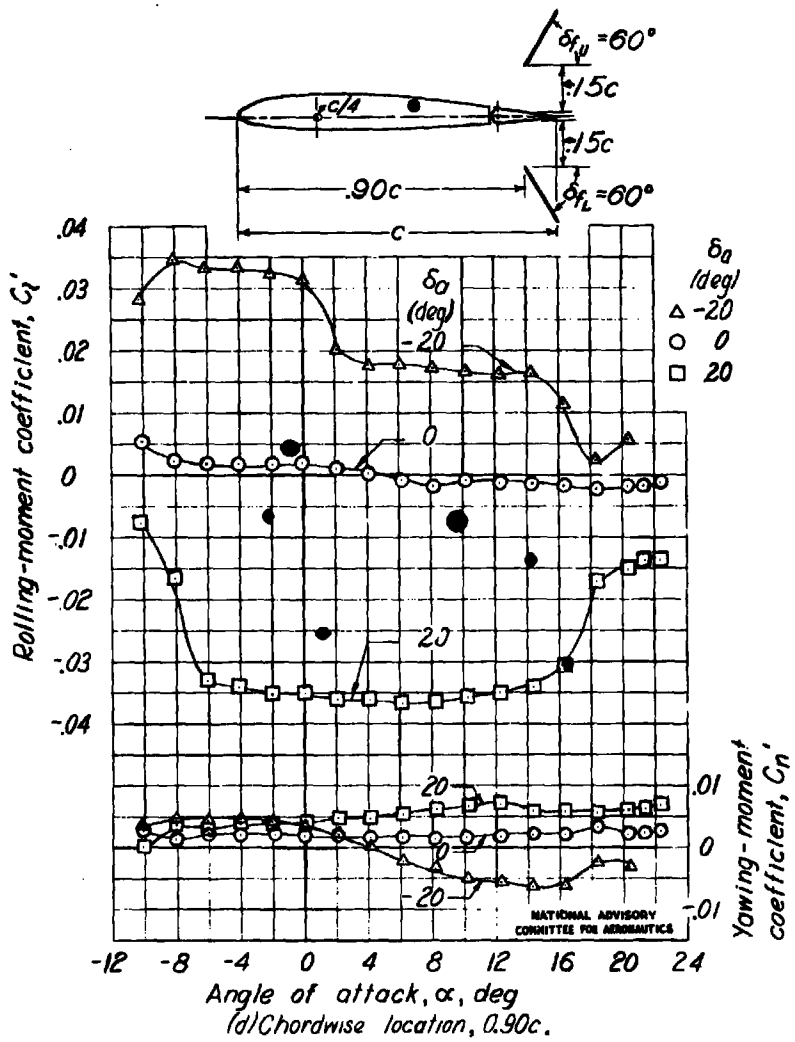

(d) Chordwise location, 0.90c.

Figure 16.- Concluded.

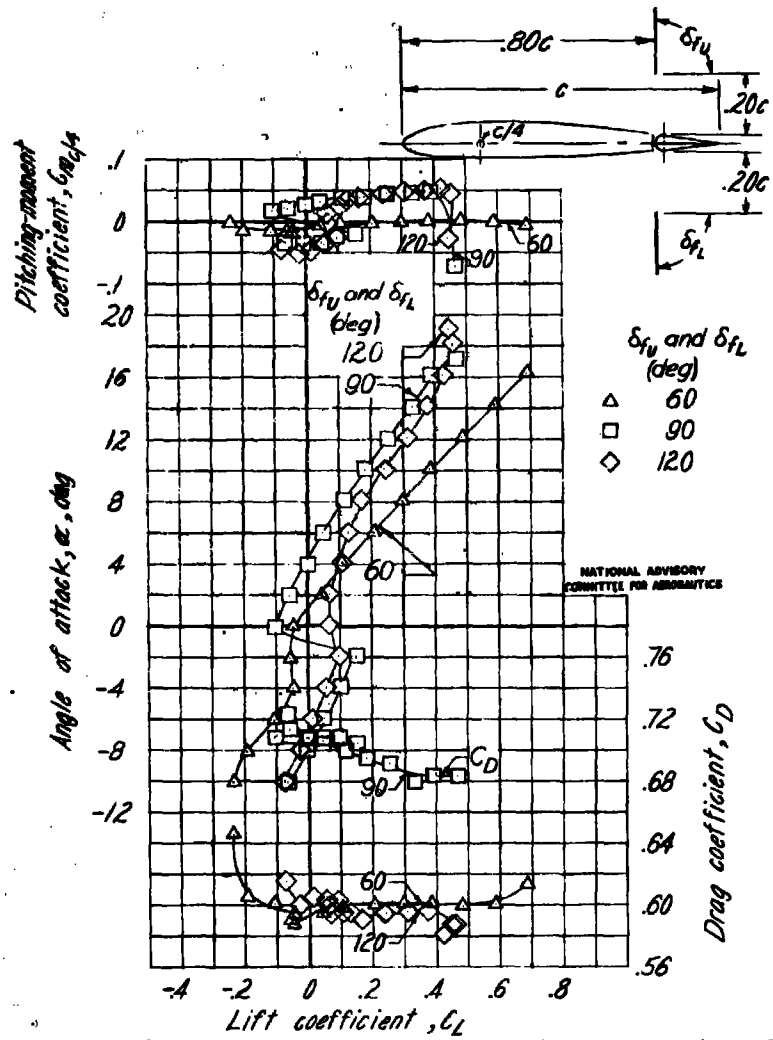

Figure 17- Lift, drag, and pitching-moment characteristics of the NACA 2212 wing model equipped with balanced double split flaps having flat-plate sections. Chordwise location, 0.80c, gaps, 0.20c; δ_0, 0°.

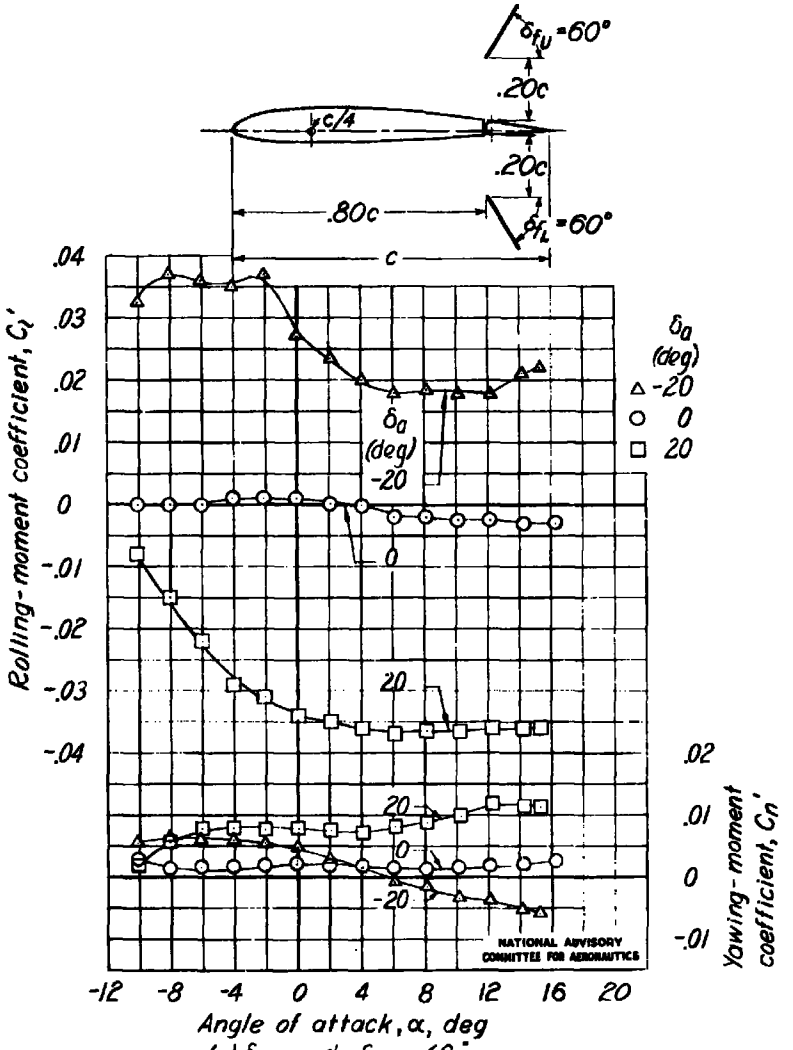

(a) δ_{f_U} and δ_{f_L}, 60°.

Figure 18.- Rolling- and yawing-moment characteristics of the right semispan aileron on the NACA 2212 wing model equipped with balanced double split flaps having flat-plate sections. Chordwise location, 0.80c, gaps, 0.20c.

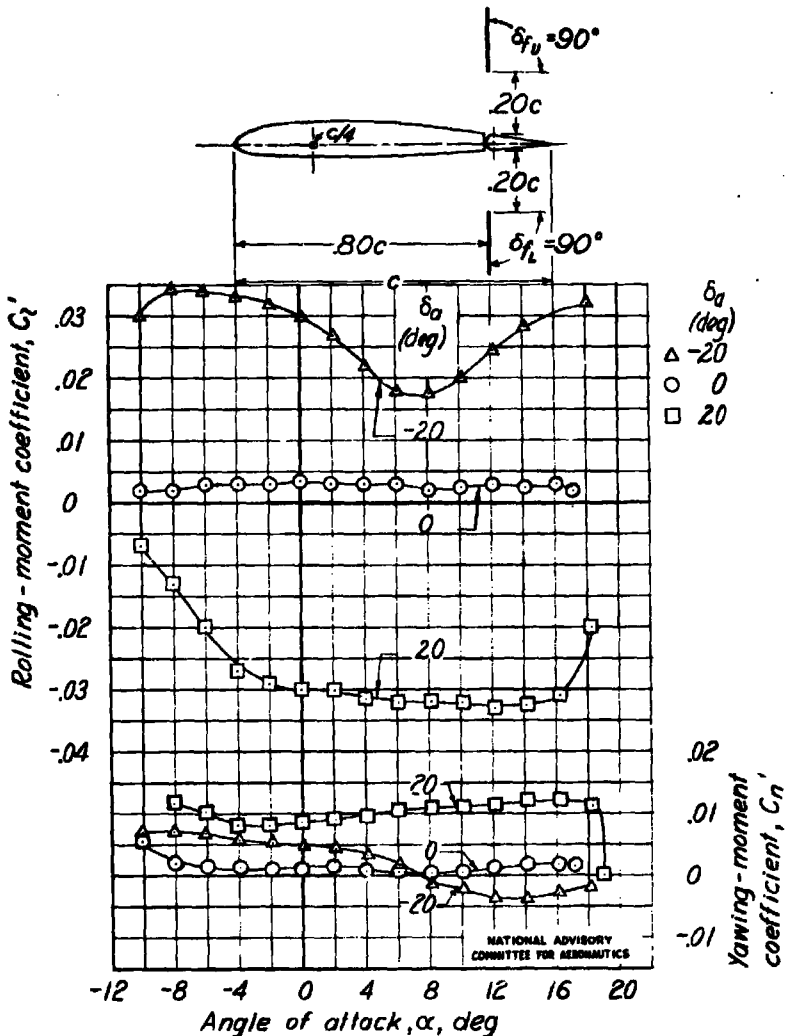

(b) δ_{f_U} and δ_{f_L}, 90°.

Figure 18.- Continued.

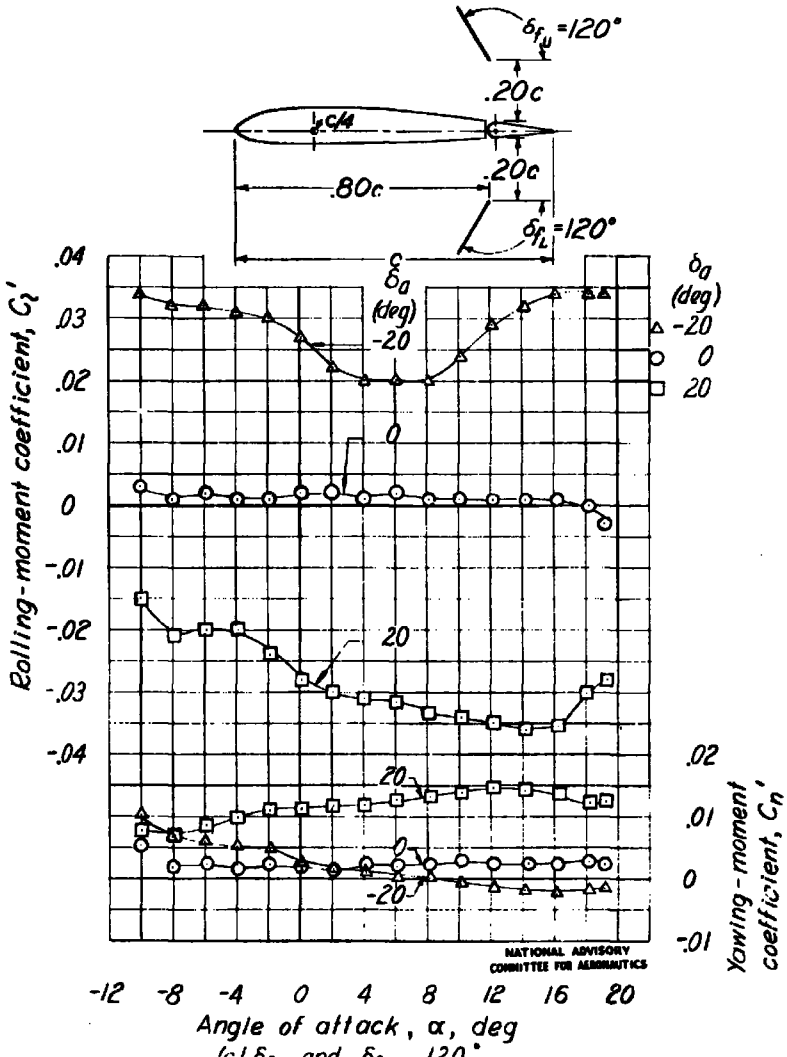

(c) δ_{f_U} and δ_{f_L}, 120°.

Figure 18.- Concluded.

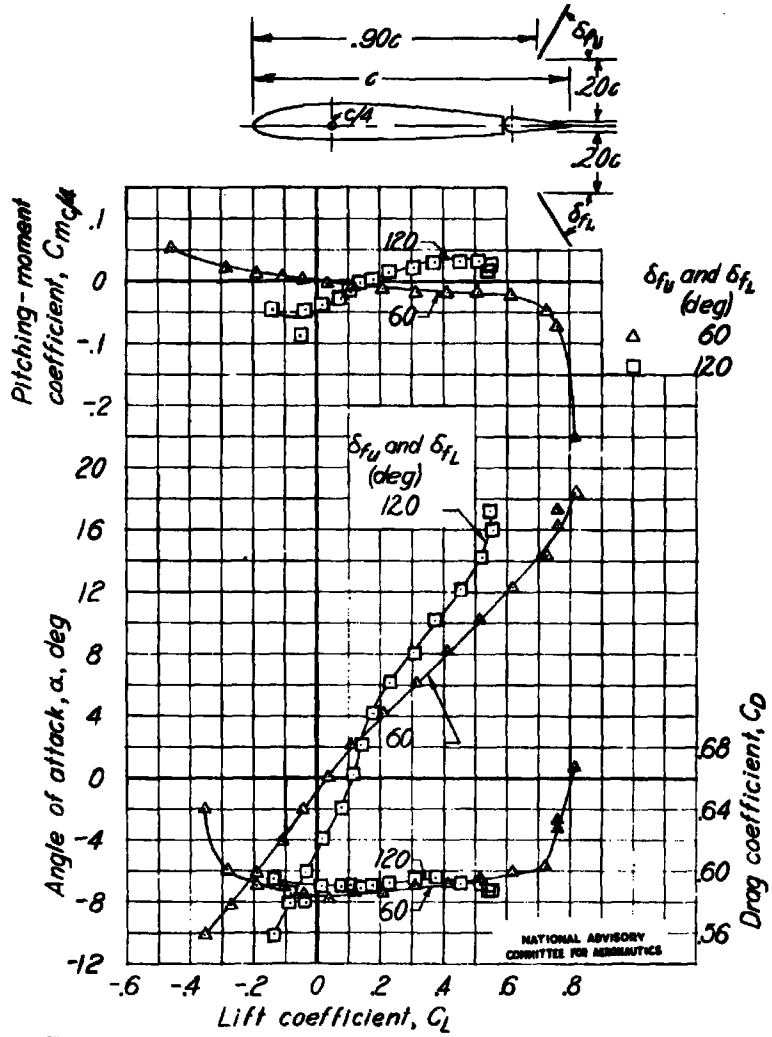

Figure 19.–Lift, drag, and pitching-moment characteristics of the NACA 2212 wing model equipped with balanced double split flaps having flat-plate sections. Chordwise location, 0.90c; gaps, 0.20c; δ_0, 0°.

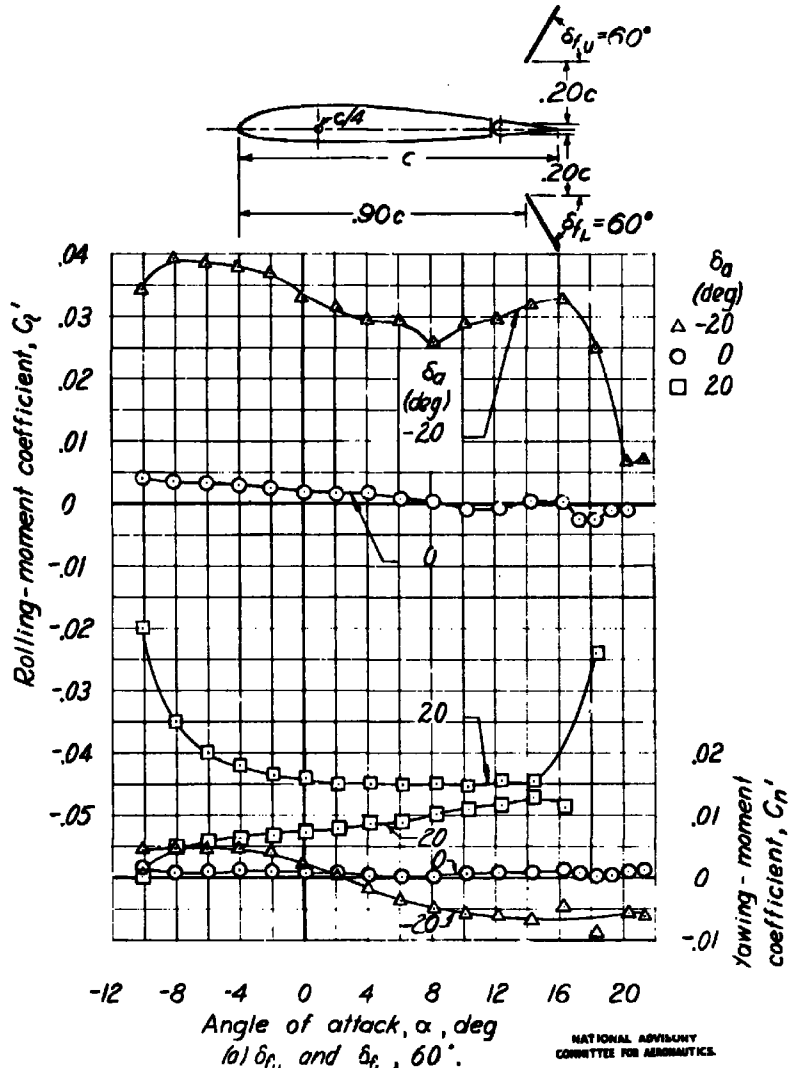

(a) δ_{f_U} and δ_{f_L}, 60°.

Figure 20.- Rolling- and yawing-moment characteristics of the right semispan aileron on the NACA 2212 wing model equipped with balanced double split flaps having flat-plate sections. Chordwise location, 0.90c; gaps, 0.20c.

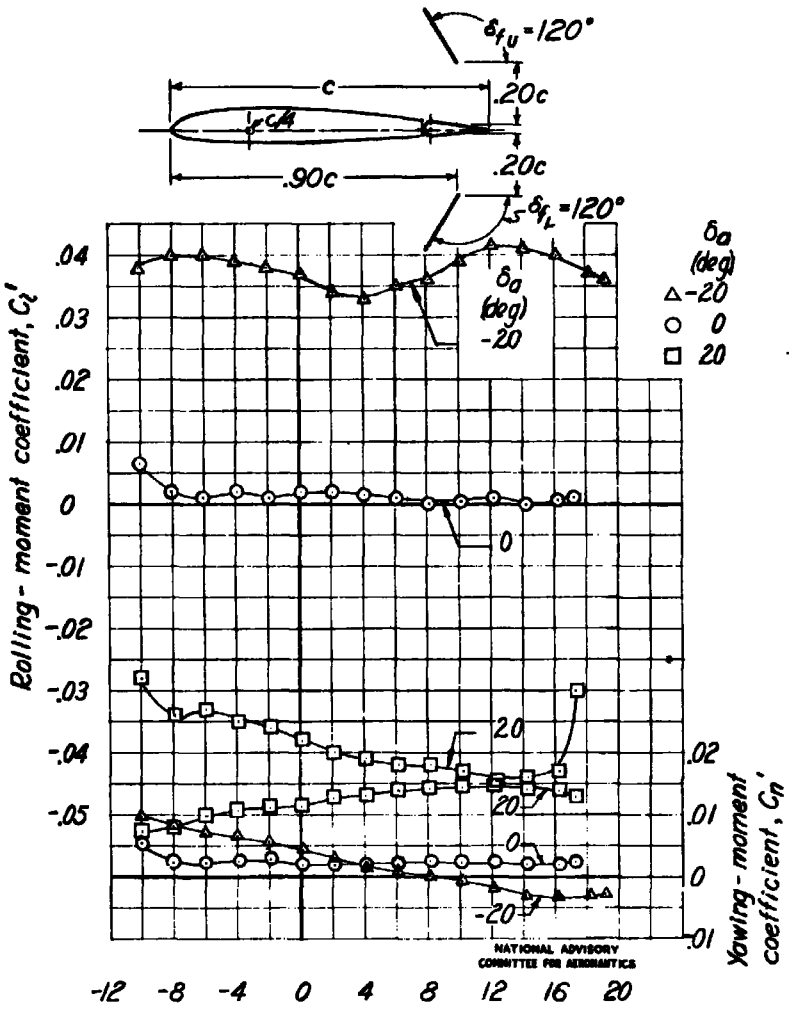

(b) δ_{f_U} and δ_{f_L}, 120°

Figure 20.- Concluded.

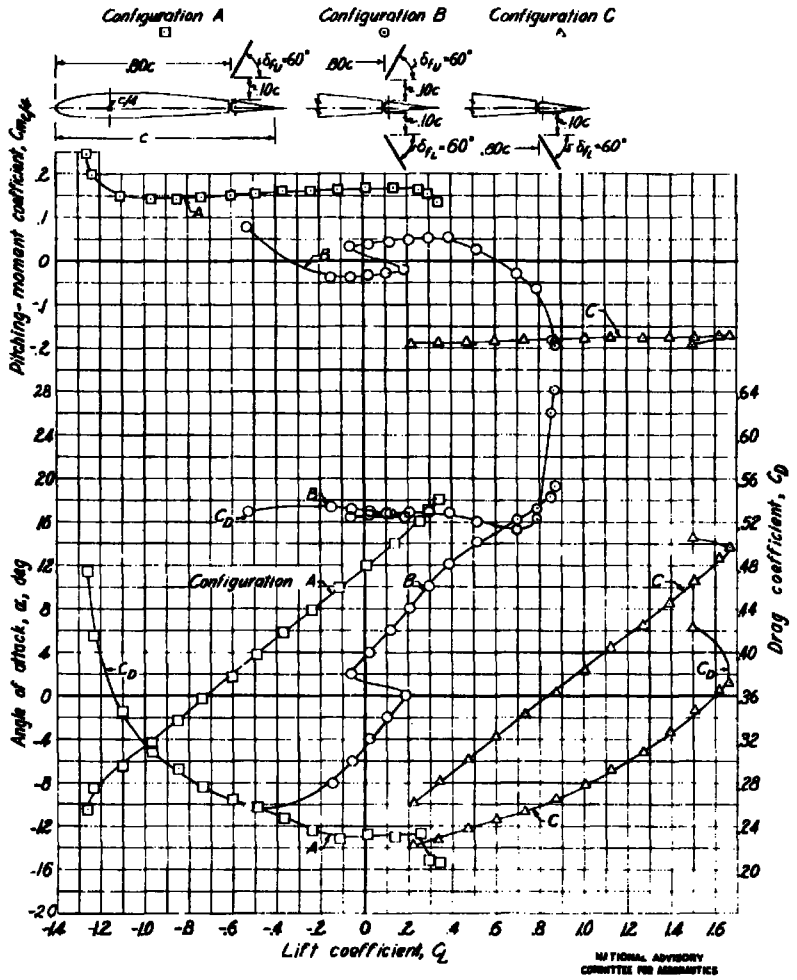

Figure 21.- Lift, drag, and pitching-moment characteristics of the NACA 2212 wing model equipped with balanced single and double split flaps having flat-plate sections. Chordwise location, 0.80c; gaps, 0.10c; δ_a, 0°; δ_{f_U} and δ_{f_L}, 60°.

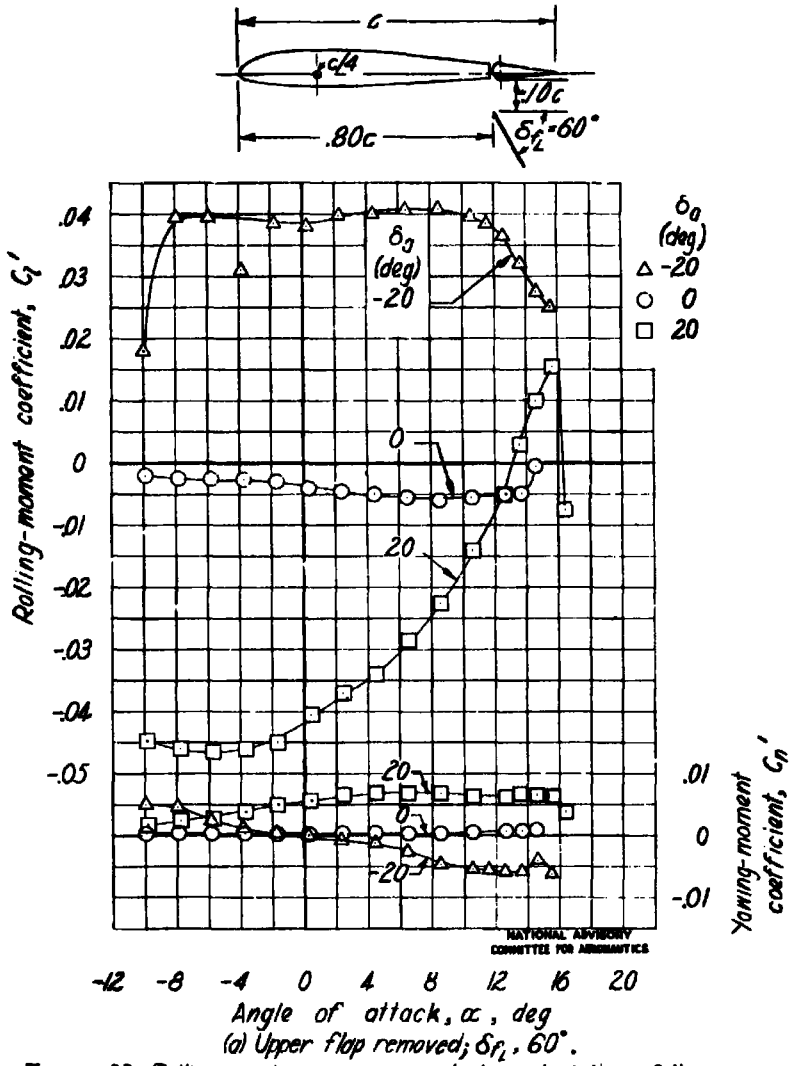

(a) Upper flap removed; δ_{f_1}, 60°.

Figure 22.-Rolling- and yawing-moment characteristics of the right semispan aileron on the NACA 2212 wing model equipped with balanced single split flap having flat-plate section. Chordwise location, 0.80c; gap, 0.10c.

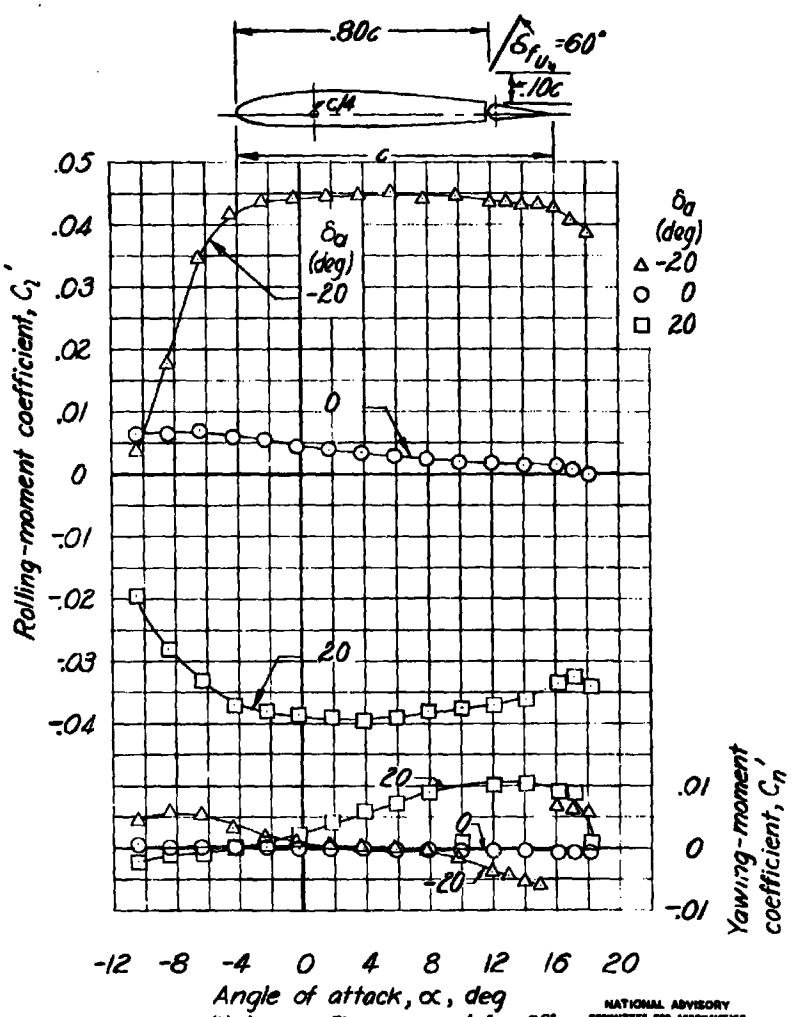

(b) Lower flap removed; δ_{f_U}, 60°.

Figure 22- Concluded.

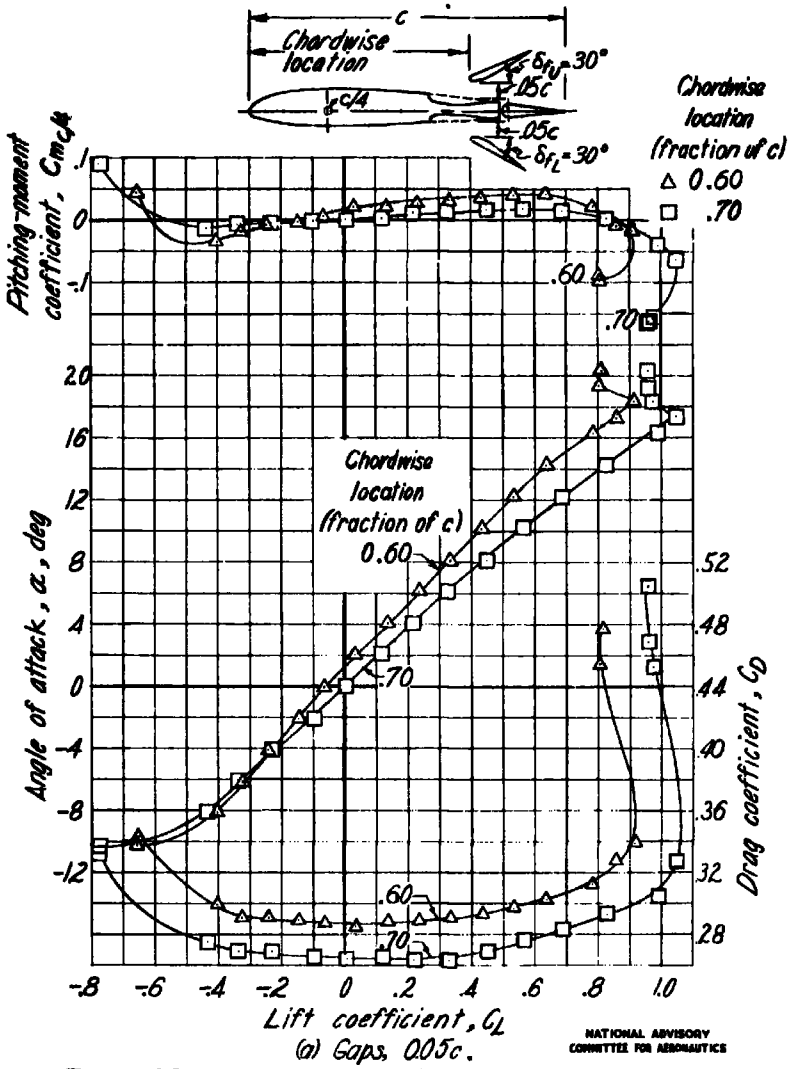

(a) Gaps, 0.05c.

Figure 23.- Lift, drag, and pitching-moment characteristics of the NACA 2212 wing model equipped with balanced double split flaps having Clark Y sections. δ_a, 0°; δ_{f_U} and δ_{f_L}, 30°.

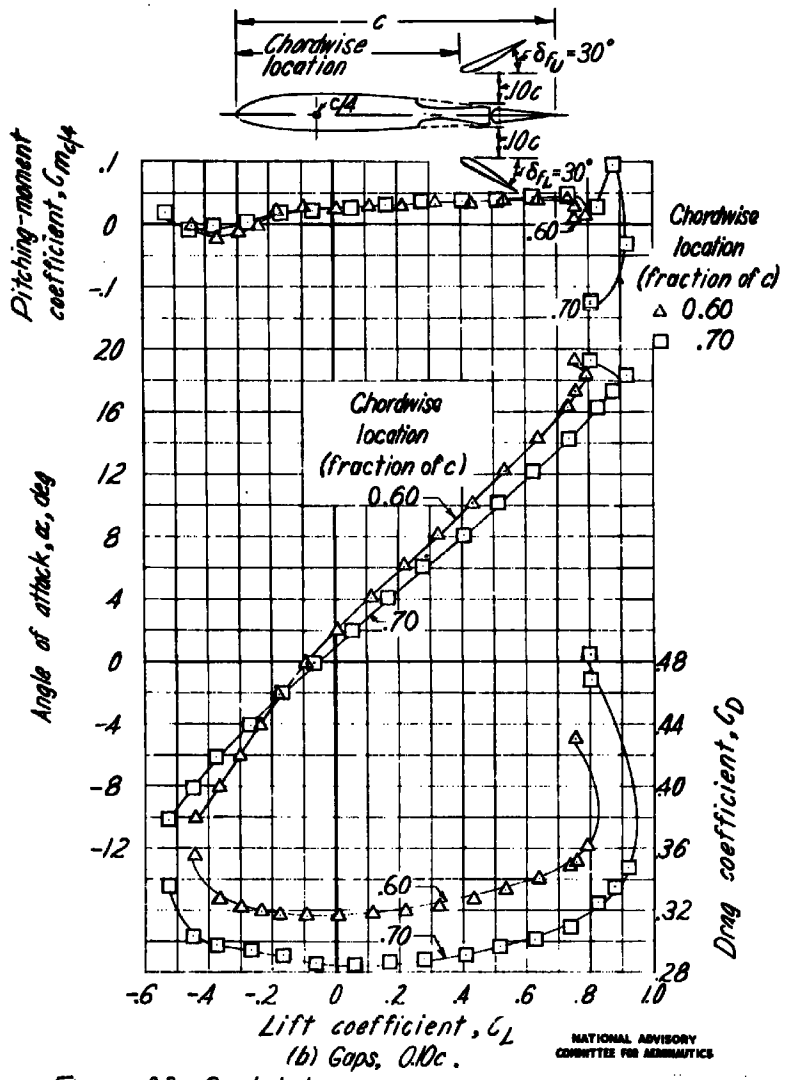

(b) Gaps, 0.10c.

Figure 23.- Concluded.

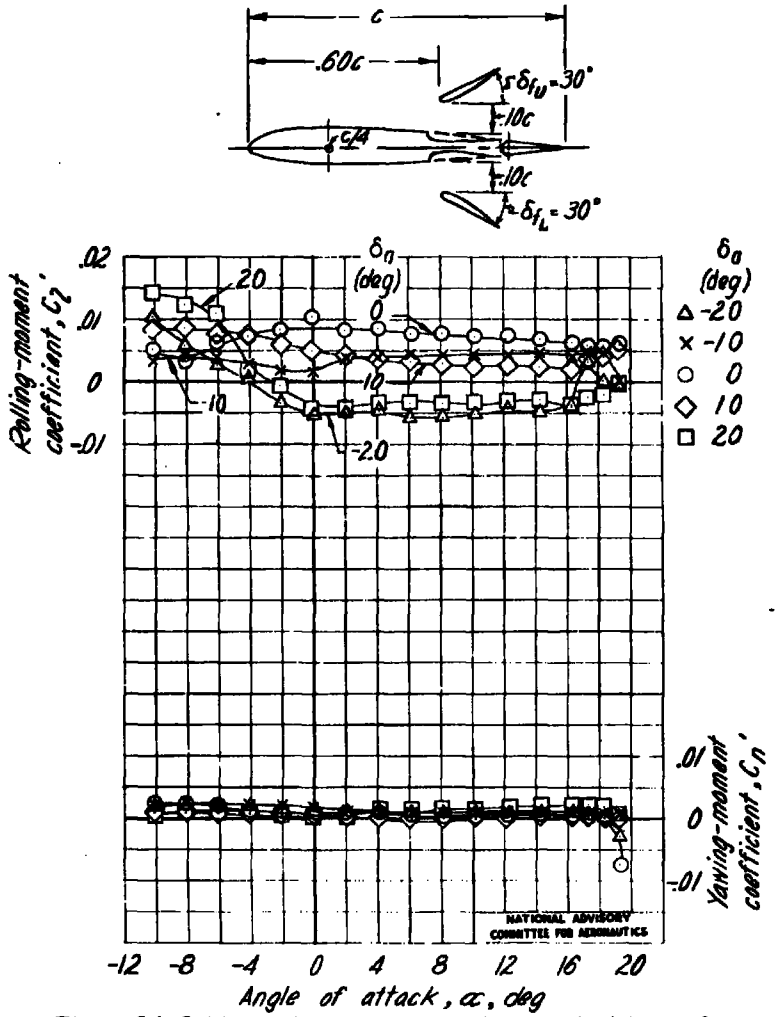

Figure 24.-Rolling-and yawing-moment characteristics of the right semispan aileron on the NACA 2212 wing model equipped with balanced double split flaps having Clark Y sections. Chordwise location, 0.60c; gaps, 0.10c; δ_{f_U} and δ_{f_L}, 30°.

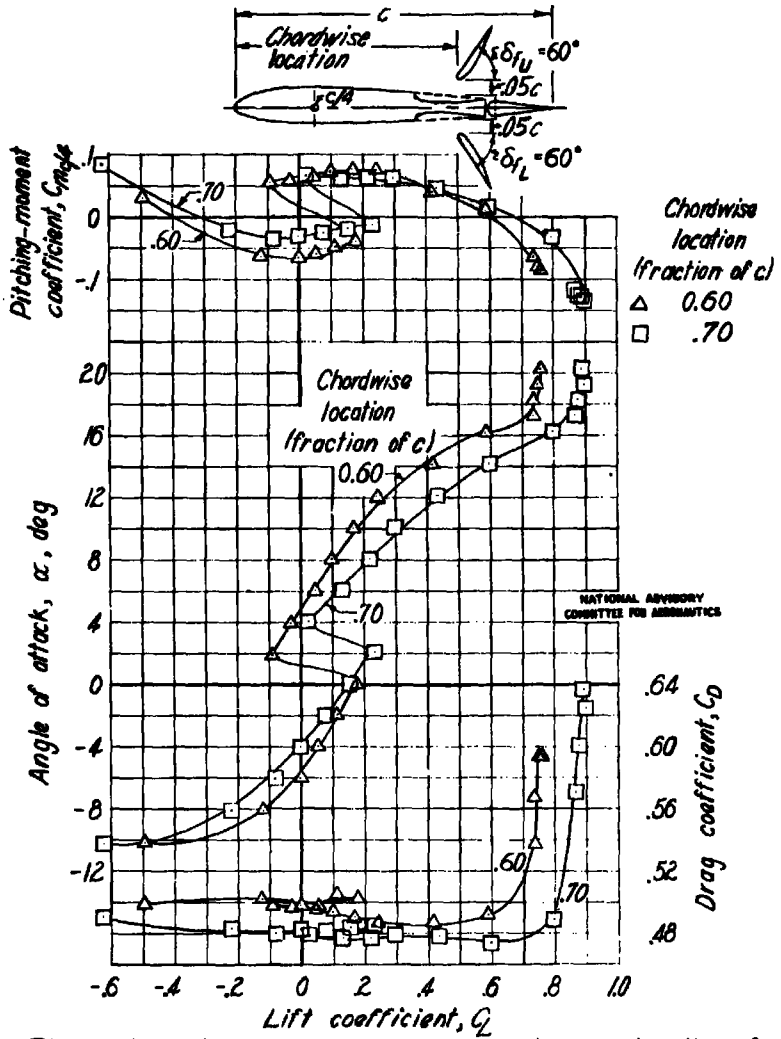

Figure 25-Lift, drag, and pitching-moment characteristics of the NACA 2212 wing model equipped with balanced double split flaps having Clark Y sections. Gaps, 0.05c; δ_a, 0°; δ_{f_U} and δ_{f_L}, 60°.

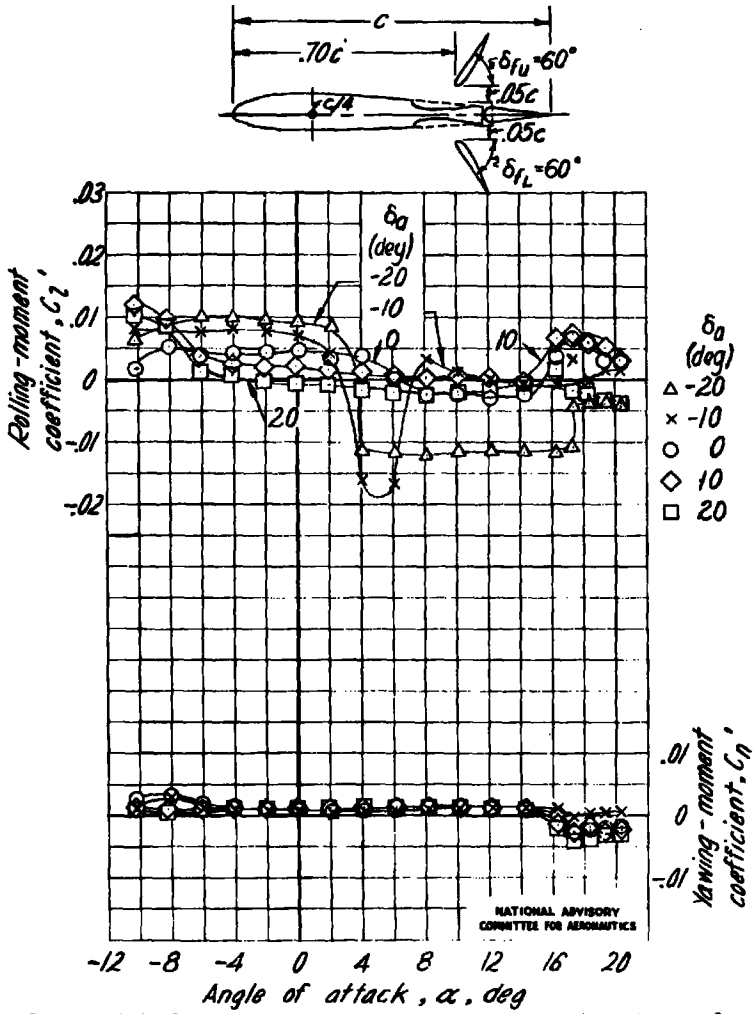

Figure 26.-Rolling-and yawing-moment characteristics of the right semispan aileron on the NACA 2212 wing model equipped with balanced double split flaps having Clark Y sections. Chordwise location, 0.70c; gaps, 0.05c; δ_{f_U} and δ_{f_L}, 60°.

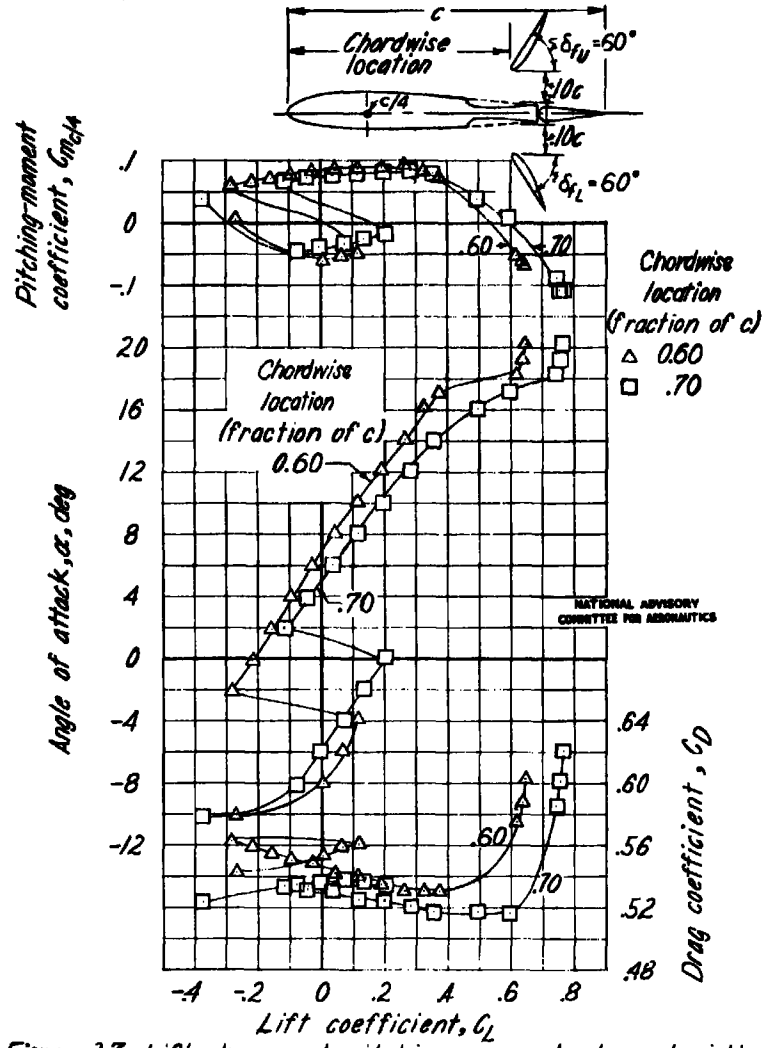

Figure 27.- Lift, drag, and pitching-moment characteristics of the NACA 2212 wing model equipped with balanced double split flaps having Clark Y sections. Gaps, 0.10c; δ_a, 0°; δ_{f_U} and δ_{f_L}, 60°.

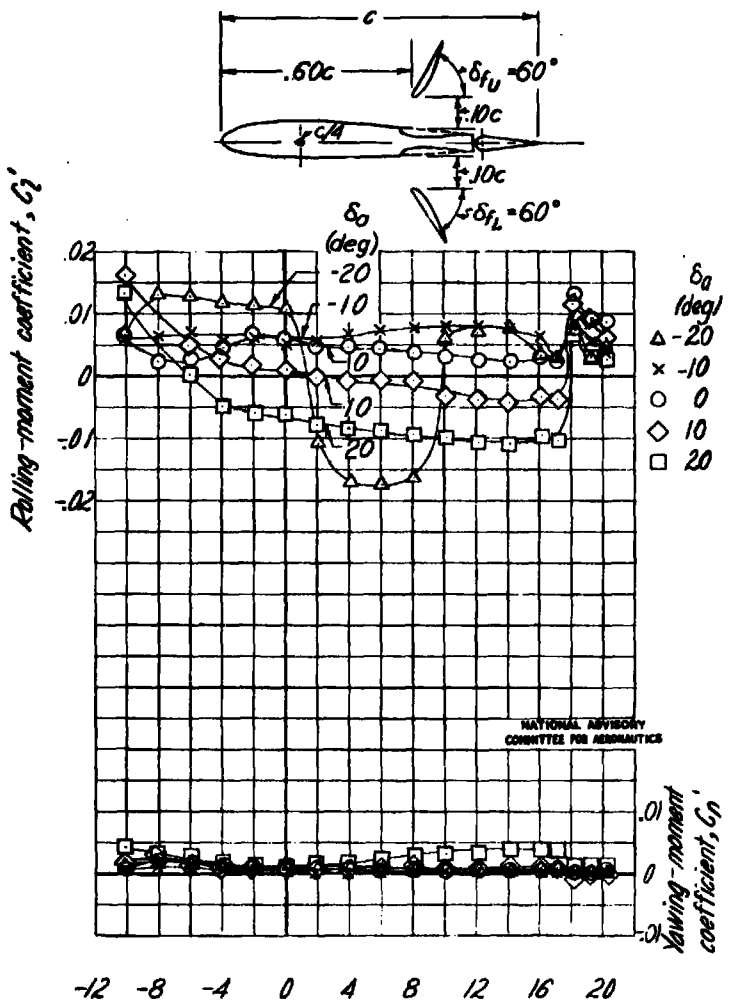

(a) Chordwise location, 0.60c.

Figure 28.- Rolling- and yawing-moment characteristics of the right semispan aileron on the NACA 2212 wing model equipped with balanced double split flaps having Clark Y sections. Gaps, 0.10c, δ_{f_U} and δ_{f_L}, 60°.

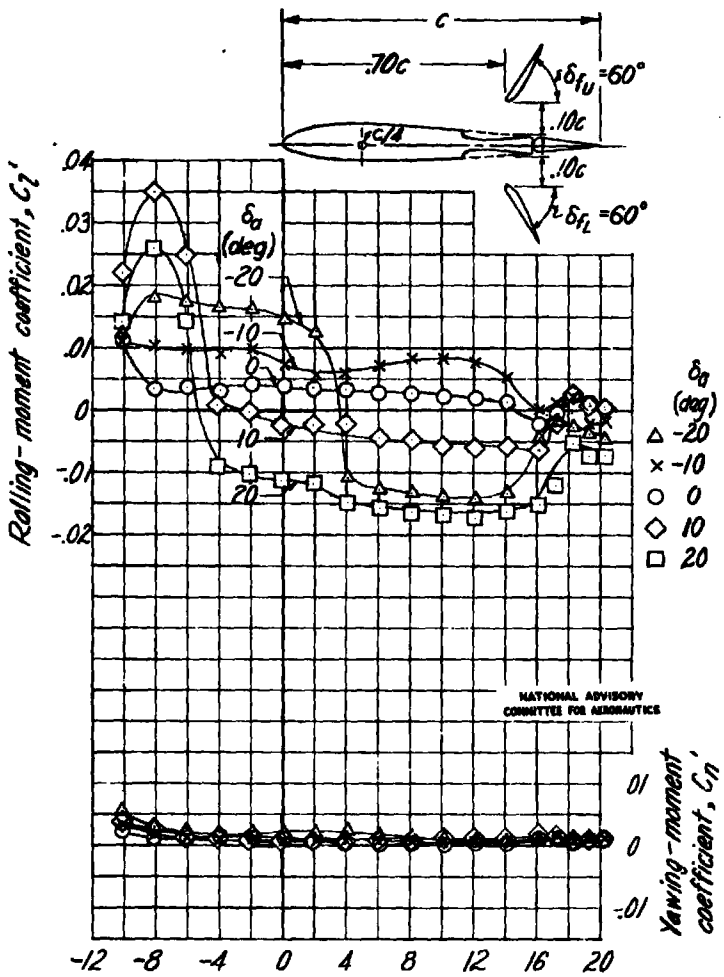

(b) Chordwise location, 0.70c.

Figure 28.- Concluded.

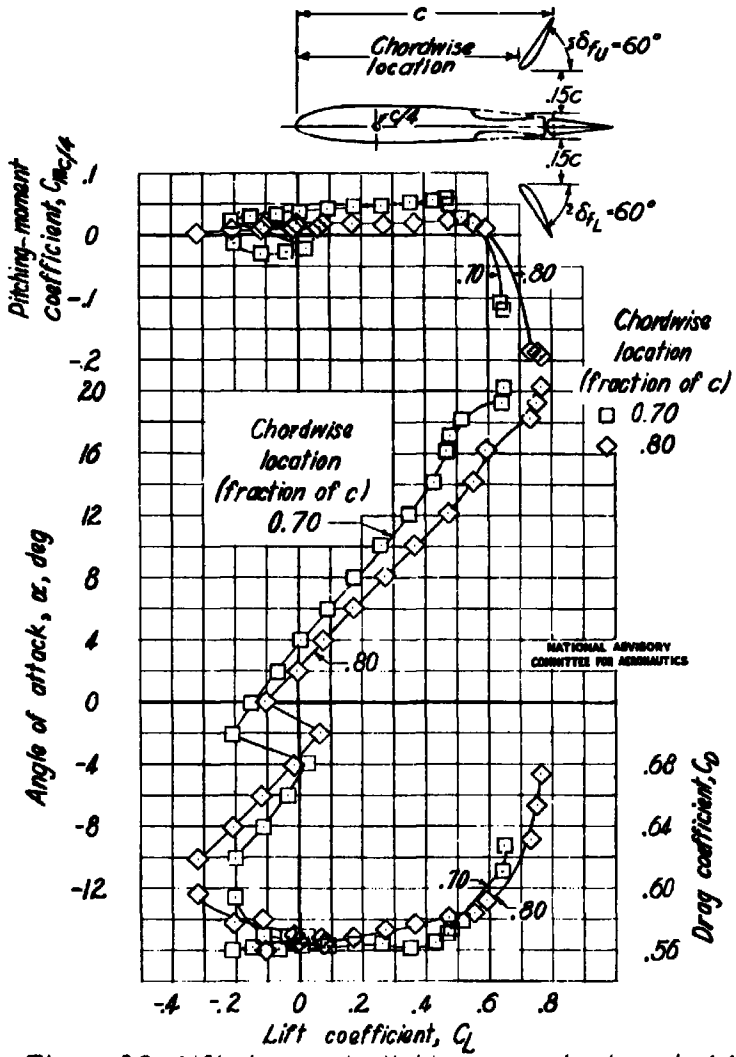

Figure 29 - Lift, drag, and pitching-moment characteristics of the NACA 2212 wing model equipped with balanced double split flaps having Clark Y sections. Gaps, 0.15c, δ_a, 0°; δ_{f_U} and δ_{f_L}, 60°.

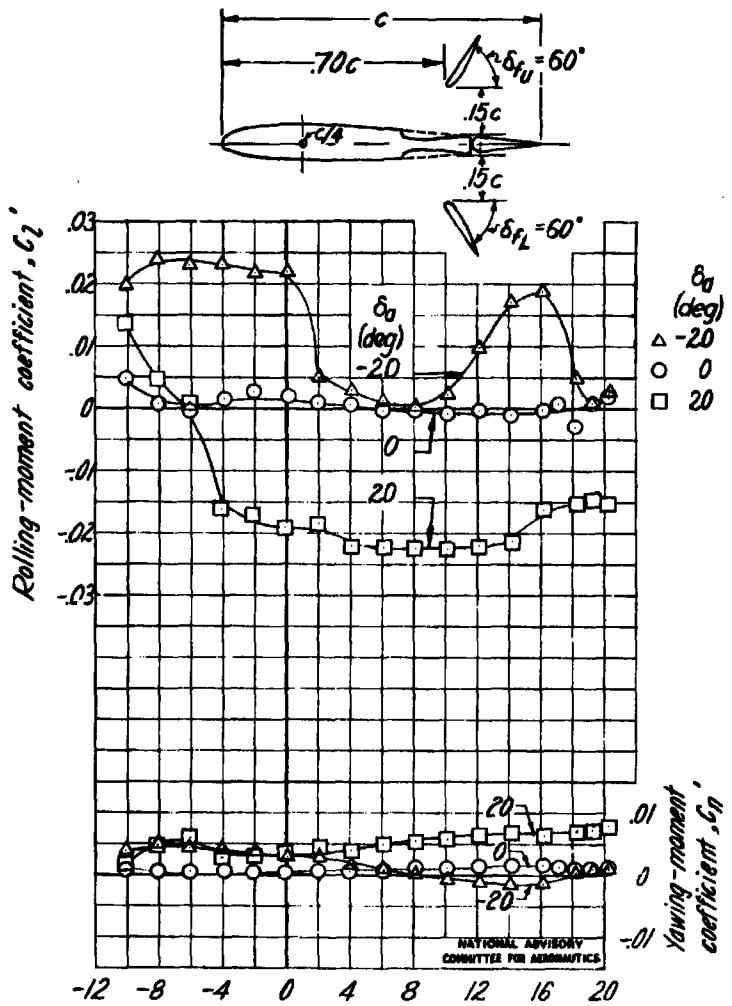

(a) Chordwise location, 0.70c.

Figure 30.- Rolling- and yawing-moment characteristics of the right semispan aileron on the NACA 2212 wing model equipped with balanced double split flaps having Clark Y sections. Gaps, 0.15c; δ_{f_U} and δ_{f_L}, 60°.

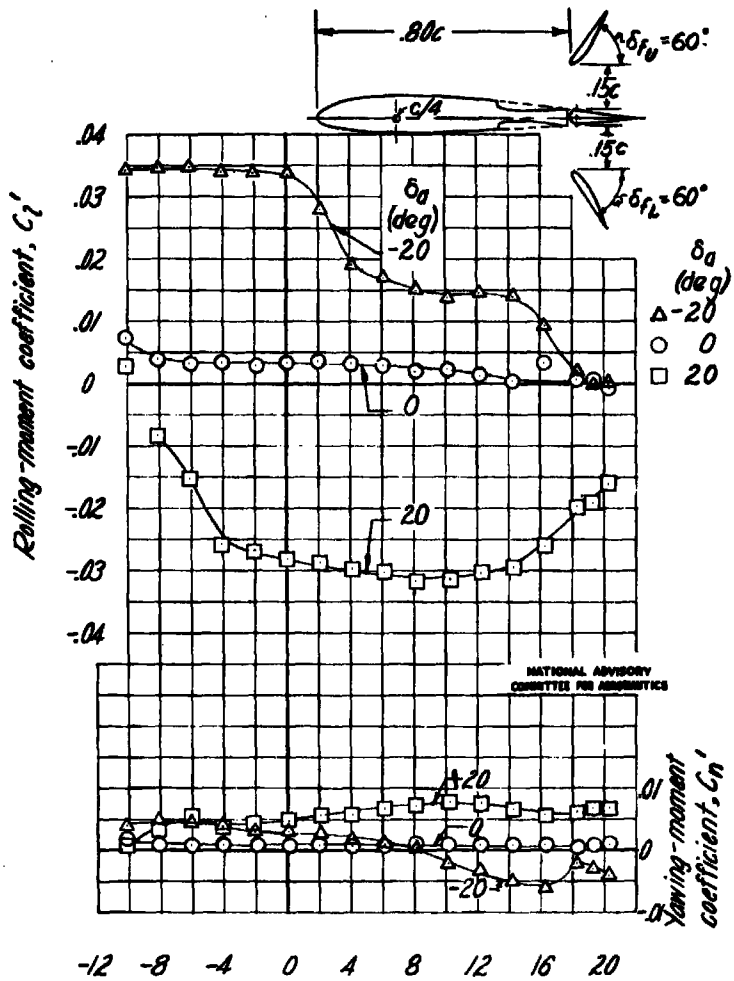

(b) Chordwise location, 0.80c.

Figure 30.– Concluded.

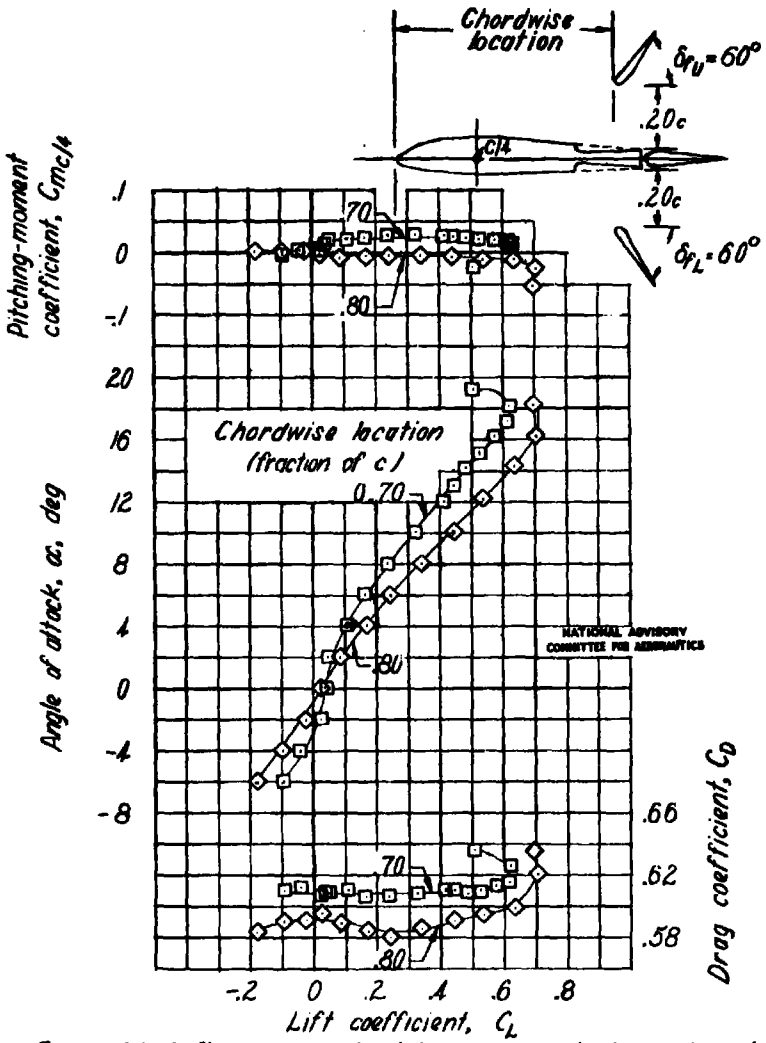

Figure 31.- Lift, drag, and pitching-moment characteristics of the NACA 2212 wing model equipped with balanced double split flaps having Clark Y sections. Gaps, 0.20c; δ_a, 0°; δ_{f_U} and δ_{f_L}, 60°.

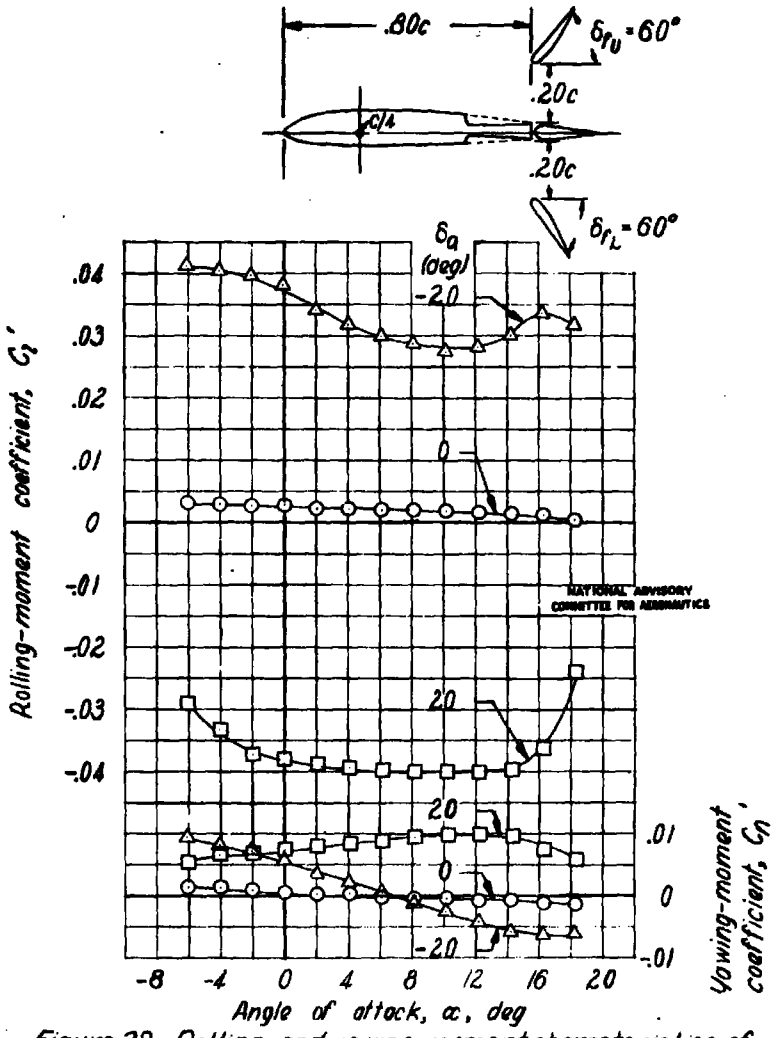

Figure 32.-Rolling-and yawing-moment characteristics of the right semispan aileron on the NACA 2212 wing model equipped with balanced double split flaps having Clark Y sections. Chordwise location, 0.80c; gaps, 0.20c; δ_{f_U} and δ_{f_L}, 60°.

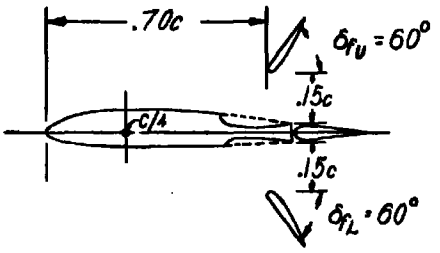

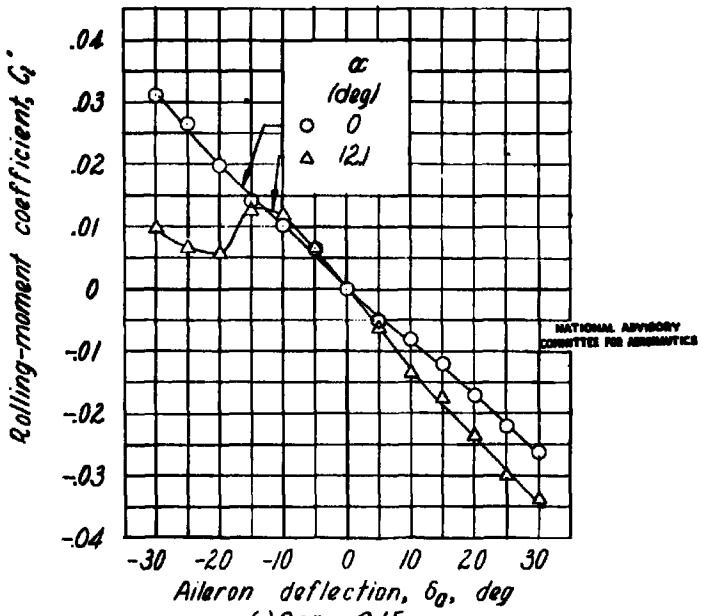

(a) Gaps, 0.15c.

Figure 33.-Rolling-moment characteristics of the right semispan aileron on the NACA 2212 wing model equipped with balanced double split flaps having Clark Y sections. Chordwise location, 0.70c; δ_{f_U} and δ_{f_L}, 60°.

(38)

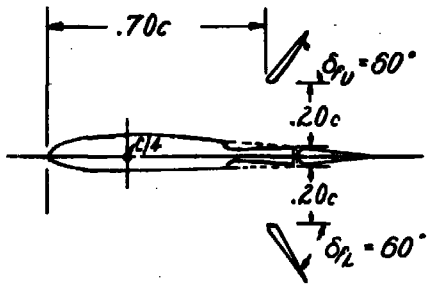

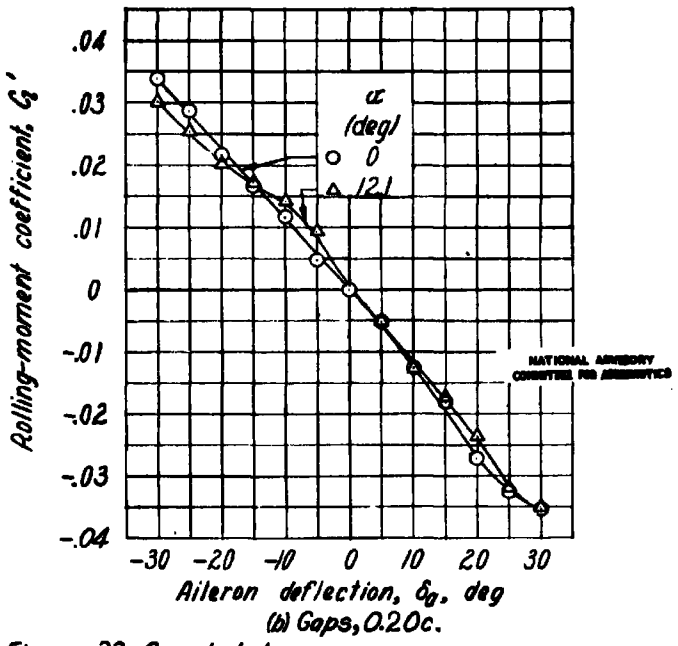

(b) Gaps, 0.20c.

Figure 33.- Concluded.

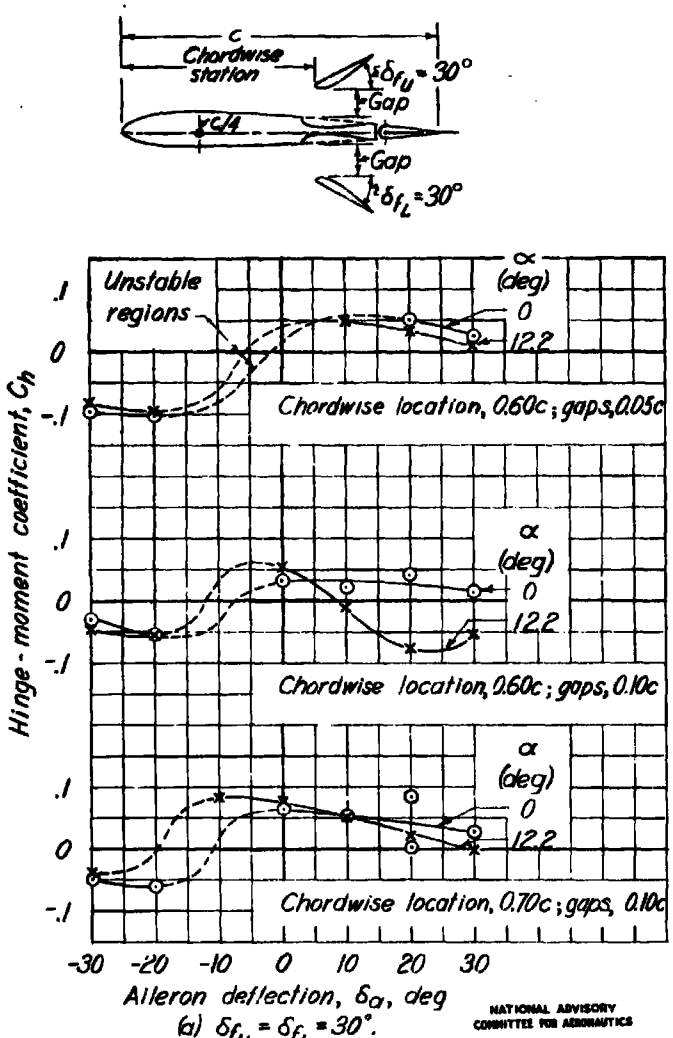

(a) $\delta_{f_U} = \delta_{f_L} = 30°$.

Figure 34-Hinge-moment characteristics of the right semispan aileron on the NACA 2.2/2 wing model equipped with balanced double split flaps having Clark Y sections.

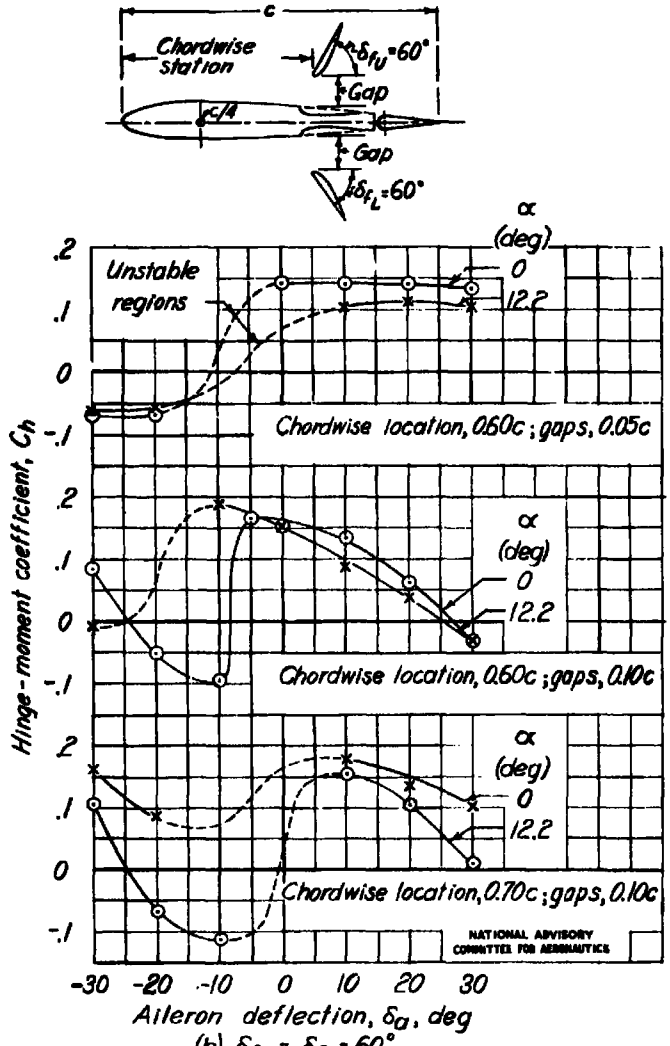

(b) $\delta_{f_U} = \delta_{f_L} = 60°$.

Figure 34.- Concluded.

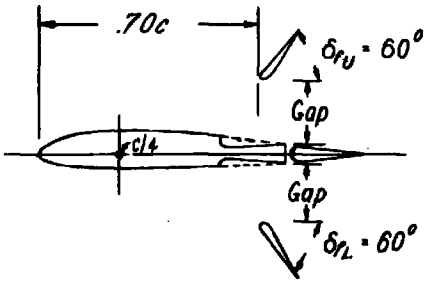

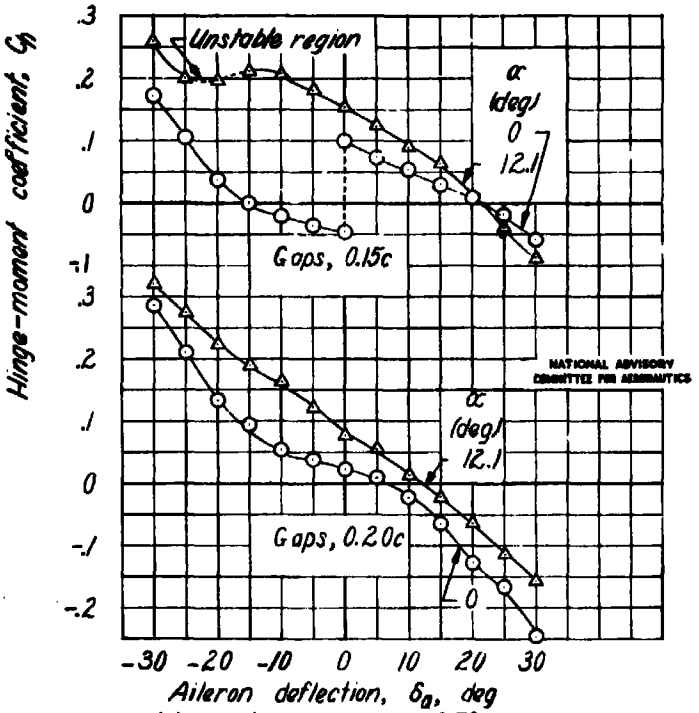

(a) Chordwise location, 0.70c.

Figure 35.-Hinge-moment characteristics of the right semi-span aileron on the NACA 2212 wing model equipped with balanced double split flaps having Clark Y sections. δ_{fU} and δ_{fL}, 60°.

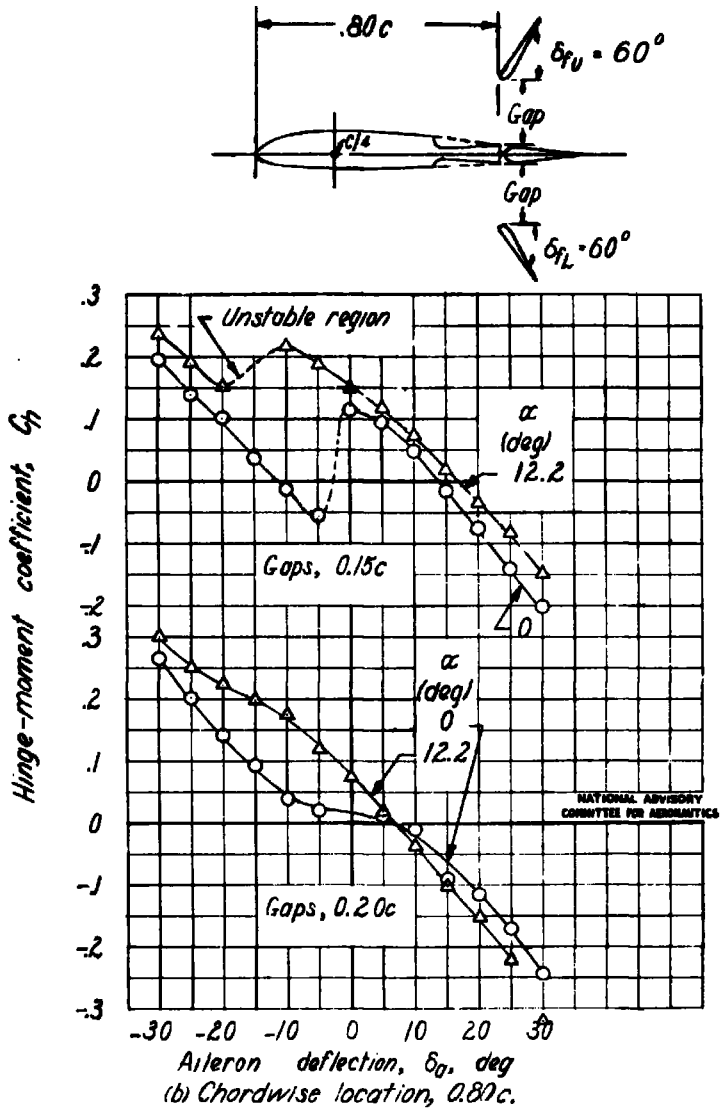

(b) Chordwise location, 0.80c.

Figure 35.- Concluded.

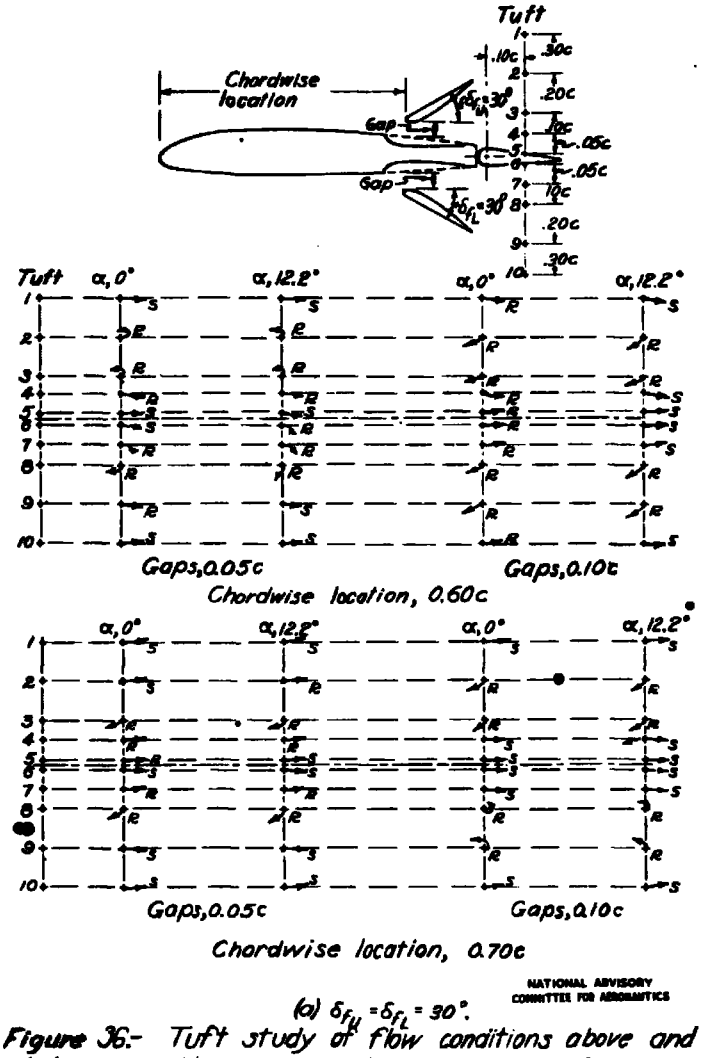

(a) $\delta_{f_u} = \delta_{f_l} = 30°$.

NATIONAL ADVISORY COMMITTEE FOR AERONAUTICS

Figure 36.- Tuft study of flow conditions above and below the right semispan aileron on the NACA 2212 wing model equipped with balanced double split flaps having Clark Y sections. Tufts located at aileron midspan; S indicates smooth flow; R indicates rough flow.

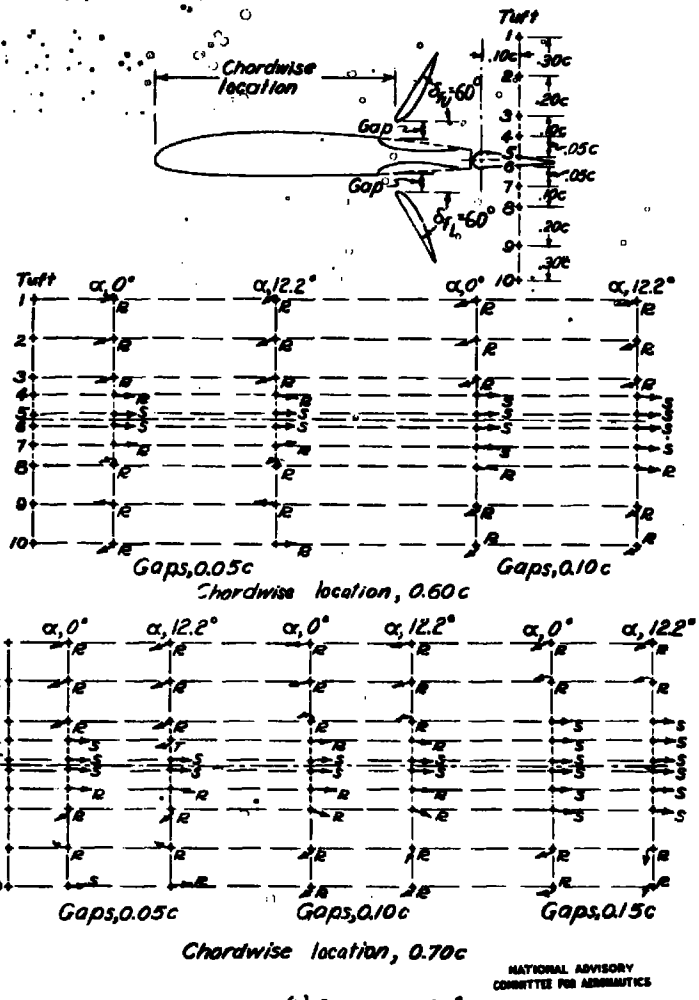

NATIONAL ADVISORY COMMITTEE FOR AERONAUTICS

(b) $\delta_{f_u} = \delta_{f_L} = 60°$.

Figure 36.- Concluded.

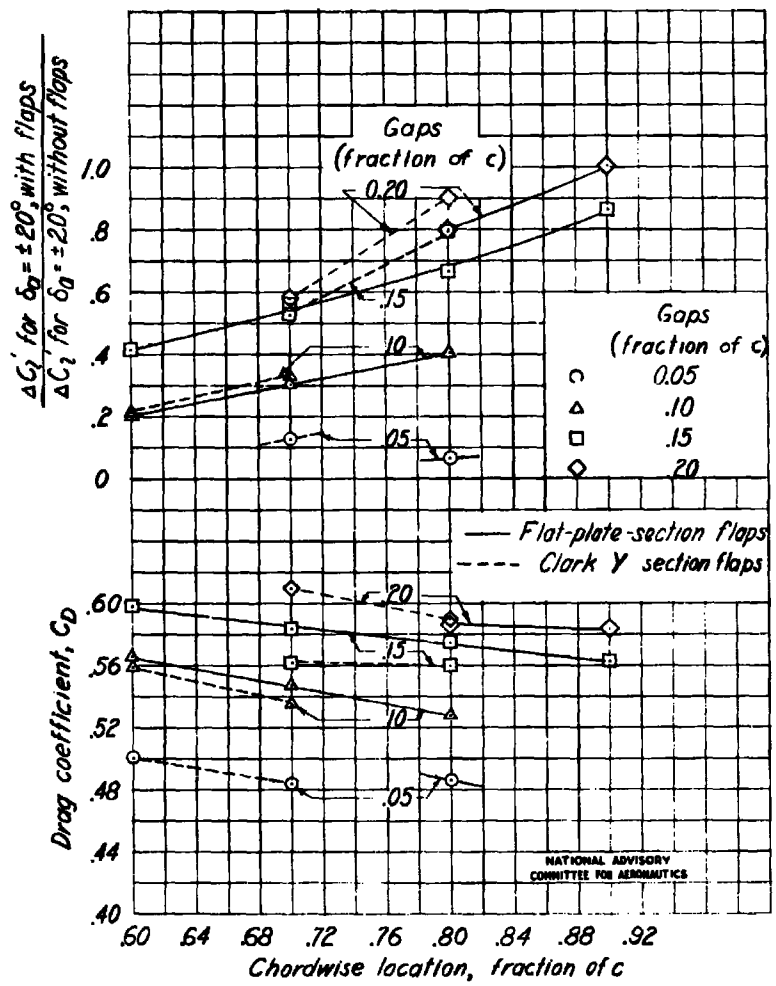

Figure 37.- Effect of chordwise location and gaps on the drag coefficients and the aileron effectiveness of the NACA 2212 wing model equipped with balanced double split flaps having flat-plate or Clark Y sections. $\alpha, 0^\circ; \delta_{f_l}$ and $\delta_{f_t}, 60^\circ$.

REEL - C

151

A.T.I.

6476

[redacted]

TITLE: Wind-Tunnel Investigation of a Rectangular NACA 2212 Airfoil with Semispan Ailerons and with Nonperforated, Balanced Double Split Flaps for Use as Aerodynamic Brakes

AUTHOR(S): Toll, Thomas A.; Ivey, Margaret

ORIGINATING AGENCY: National Advisory Committee for Aeronautics, Washington, D. C.

PUBLISHED BY: (Same)

ATI-6476

REVISION: (None)

ORIG. AGENCY NO.: ARR-L5B17

PUBLISHING AGENCY NO.:

DATE	DOC. CLASS.	COUNTRY	LANGUAGE	PAGES	ILLUSTRATIONS
April '45	[redacted]	U.S.	Eng.	41	photos, diagr, graphs

ABSTRACT:

* Flaps (Control Surfaces)

Flat-plate flaps with no wing cutouts and flaps having Clark Y sections with corresponding cutouts made in wing were tested for various flap deflections, chordwise locations, and gaps between flaps and airfoil contour. The drag was slightly lower for wing with airfoil section flaps. Satisfactory aileron effectiveness was obtained with flap gap of 20% wing chord and flap-nose location of 80% wing chord behind leading edge. Airflow was smooth and buffeting negligible.

Aerodynamic Drag P1/1

DISTRIBUTION: Request copies of this report only from Originating Agency

DIVISION: Aerodynamics ~~(2)~~

SECTION: Wings and Airfoils ~~(6)~~ 9 6-7

SUBJECT HEADINGS: Airfoil theory (06200); Flaps (37450); Control surfaces - Aerodynamics (25600); Airfoils - Drag (08200)

ATI SHEET NO.: R-2-6-51

Air Documents Division, Intelligence Department
Air Materiel Command

AIR TECHNICAL INDEX [redacted]

Wright-Patterson Air Force Base
Dayton, Ohio

RESTRICTED

TITLE: Wind-Tunnel Investigation of a Rectangular NACA 2212 Airfoil with Semispan Ailerons and with Nonperforated, Balanced Double Split Flaps for Use as Aerodynamic Brakes

AUTHOR(S): Toll, Thomas A.; Ivey, Margaret

ORIGINATING AGENCY: National Advisory Committee for Aeronautics, Washington, D. C.

PUBLISHED BY: (Same)

ATI-6476

DIVISION: (None)

ORIG. AGENCY NO.: ARR-L5B17

PUBLISHED AGENCY NO.:

DATE	DOC. CLASS.	COUNTRY	LANGUAGE	PAGES	ILLUSTRATIONS
April '45	Restr.	U.S.	Eng.	41	photos, diagr, graphs

ABSTRACT:

Flat-plate flaps with no wing cutouts and flaps having Clark Y sections with corresponding cutouts made in wing were tested for various flap deflections, chordwise locations, and gaps between flaps and airfoil contour. The drag was slightly lower for wing with airfoil section flaps. Satisfactory aileron effectiveness was obtained with flap gap of 20% wing chord and flap-nose location of 80% wing chord behind leading edge. Airflow was smooth and buffeting negligible.

DISTRIBUTION: Request copies of this report only from Originating Agency

DIVISION: Aerodynamics (2)

SECTION: Wings and Airfoils (6)

SUBJECT HEADINGS: Airfoil theory (06200); Flaps (37450); Control surfaces - Aerodynamics (25600); Airfoils - Drag (08200)

ATI SHEET NO.: R-2-6-51

Air Documents Division, Intelligence Department
Air Material Command

AIR TECHNICAL INDEX
RESTRICTED

Wright-Patterson Air Force Base
Dayton, Ohio